Characterization of organic nitrogen in aerosols at a forest site in the southern Appalachian Mountains

Xi Chen[1], Mingjie Xie[2,a], Michael D. Hays[1], Eric Edgerton[3], Donna Schwede[4], John T. Walker[1,*]

[1]National Risk Management Research Laboratory, Office of Research and Development, U.S. Environmental Protection Agency, Research Triangle Park, North Carolina, 27711, U.S.A.

[2]Oak Ridge Institute for Science and Education (ORISE), National Risk Management Research Laboratory, Office of Research and Development, U.S. Environmental Protection Agency, Research Triangle Park, North Carolina, 27711, U.S.A.

[3]Atmospheric Research and Analysis, Inc., Cary, NC, 27513

[4]National Exposure Research Laboratory, Office of Research and Development, U.S. Environmental Protection Agency, Research Triangle Park, North Carolina, 27711, U.S.A.

[a]Present address: School of Environmental Science and Engineering, Nanjing University of Information Science & Technology, Nanjing 210044, China

[*]Corresponding Author: Tel.: +1 919 541 2288. Email:Walker.JohnT@epa.gov.

Abstract

This study investigates the composition of organic particulate matter in $PM_{2.5}$ in a remote montane forest in the southeastern U.S., focusing on the role of organic nitrogen (N) in sulfur-containing secondary organic aerosol (nitrooxy-organosulfates) and aerosols associated with biomass burning (nitro-aromatics). Bulk water soluble organic N (WSON) represented ~ 14% w/w of water soluble total N (WSTN) in $PM_{2.5}$, on average, across seasonal measurement campaigns conducted in the spring, summer, and fall of 2015. Largest contributions of WSON to WSTN were observed in spring (~ 18% w/w) and lowest in the fall (~10% w/w). On average, identified nitro-aromatic and nitrooxy-organosulfate compounds accounted for a small fraction of WSON, ranging from ~ 1% in spring to ~ 4% in fall, though were observed to contribute as much as 28% w/w of WSON in individual samples which were impacted by local biomass burning. Highest concentrations of oxidized organic N species occurred during summer (average of 0.65ngN/m^3) along with a greater relative abundance of higher generation oxygenated

terpenoic acids, indicating an association with more aged aerosol. Highest concentrations of nitro-aromatics (eg. nitrocatechol and methyl-nitrocatechol), levoglucosan, and aged SOA tracers were observed during fall, associated with aged biomass burning plumes. Nighttime nitrate radical chemistry is the most likely formation pathway for nitrooxy-organosulfates observed at this low NOx site (generally <1ppb). Isoprene derived organosulfate (MW216, 2-methyltetrol derived), which is formed from isoprene epoxydiols (IEPOX) under low NOx conditions, was the most abundant individual organosulfate. Concentration weighted average WSON/WSOC ratios for nitro-aromatics + organosulfates + terpenoic acids were one order of magnitude lower than the overall aerosol WSON/WSOC ratio, indicating the presence of other uncharacterized higher N content species. Although nitrooxy-organosulfates and nitro-aromatics contributed a small fraction of WSON, our results provide new insight into the atmospheric formation processes and sources of these largely uncharacterized components of atmospheric organic N, which also helps to advance the atmospheric models to better understand the chemistry and deposition of reactive N.

1. Introduction

There is extensive evidence showing that boreal and temperate forests are affected by anthropogenic activities, both industrial and agricultural. Such activity results in unprecedented quantities of reactive nitrogen (N) being released into the atmosphere, subsequently altering global nitrogen and carbon (C) biogeochemical cycles (Bragazza et al., 2006; Doney et al., 2007; Ollinger et al., 2002; Magnani et al., 2007; Neff et al., 2002a,b; Pregitzer et al., 2008). Nitrogen enters natural ecosystems through atmospheric deposition and biological fixation, and is mainly lost through leaching and gaseous fluxes back to the atmosphere (Hungate et al., 2003). Atmospheric deposition of N to terrestrial ecosystems may lead to soil and aquatic acidification, nutrient imbalance and enrichment, plant damage and microbial community changes as well as loss of biodiversity (Bobbink et al., 1998; Magnani et al., 2007; Lohse et al, 2008; Simkin et al., 2016).

In the United States, deposition of atmospheric pollutants including N is monitored by the National Atmospheric Deposition Program (NADP) and EPA's Clean Air Status and Trends Network (CASNET). However, these networks focus only on inorganic N species (eg. NH_3/NH_4^+ and HNO_3/NO_3^-). Recent studies shed light on the importance of organic N

deposition, which is not routinely measured in national networks. On a global basis, organic N may contribute ~ 25 percent of the total N deposition (Gonzalez Benitez et al., 2009; Jickells et al., 2013; Kanakidou et al., 2012; Keene et al., 2002; Neff et al., 2002a; Zhang et al., 2012). Although ubiquitous, widespread routine monitoring of organic N in the atmosphere is inhibited due to difficulties in sampling (Walker et al, 2012) and inability to fully speciate the wide range of constituents that make up this large pool of atmospheric N (Altieri et al., 2009, 2012; Cape et al., 2011; Neff et al., 2002a; Samy et al., 2013). For these reasons, understanding of the sources, atmospheric chemistry, and deposition of organic nitrogen remains limited.

Atmospheric N from biogenic and anthropogenic emissions sources undergoes complex transformation processes and photochemical reactions. Consequently, apportionment of atmospheric organic N to potential sources is challenging. However, such information is required to advance atmospheric N models applied to better understand the global N cycle. For example, Miyazaki et al. (2014) examined aerosols collected in a deciduous forest and found in the summer that water soluble organic N (WSON) correlated positively to biogenic hydrocarbon oxidation; and during fall WSON in the coarse particle fraction was associated with primary biological emissions (e.g. emitted from soil, vegetation, pollen and bacteria). Such patterns underscore that atmospheric organic N measured in forested landscapes originates from a variety of sources that contribute differently across seasons.

Recent advancements have been made in speciation of organic N in aerosol for some groups of compounds including amines, amino acids and other nitrogenated functional groups such as organonitrates (Day et al., 2010; Place et al., 2017; Samy et al., 2013). Organic N in secondary aerosol and aerosols associated with biomass burning sources are areas of increasing interest, from both atmospheric chemistry and ecosystem exposure perspectives, where more information is needed. Studies of secondary organic aerosols (SOA) have identified a variety of nitrated organosulfate compounds (e.g. nitrooxy-organosulfates) in both chamber and ambient aerosol samples following isoprene and monoterpenes oxidation. These compounds are either produced under high NOx conditions or from nighttime NO_3 radical chemistry (Surratt et al., 2006, 2007, 2008, 2010; Darer et al., 2011; Lin et al., 2013a; He et al., 2014; Worton et al., 2013). Potential SOA precursors such as unsaturated green leaf volatiles (GLVs) released by wounded plants (e.g. crop harvesting and insect attacks) may contribute substantially to the budget of biogenic SOA formation especially in remote forests (Gomez-Gonzalez et al., 2008;

Hamilton et al., 2013; Shalamzari et al., 2016). The detection of reaction products such as organosulfates and nitrooxy-organosulfates in ambient aerosols provides strong evidence of influence from anthropogenic sources (e.g. SO_2 and NOx) interacting with biogenic precursors to form nitrogenated SOA (Chan et al., 2010; Lin et al., 2013a; Meade et al., 2016).

In addition to being present in sulfur-containing SOA, organic nitrogen, specifically nitro-aromatic compounds (e.g.nitrophenols and nitrocatechols), have been characterized as chemical tracers from biomass burning (e.g. wildland and prescribed smoke, bushfires, residential wood burning). This is in addition to levoglucosan, a widely used tracer of biomass burning (Iinuma et al., 2010, 2016; Kahnt et al., 2013; Kitanovski et al., 2012; Gaston et al., 2016). These nitrated compounds can form during pyrolysis of plant biopolymers such as cellulose. Furthermore, as combustion byproducts, these compounds are often defined as brown carbon (BrC) and thus potentially light absorbing (Mohr et al., 2013; Liu et al., 2015). Presumably, nitro-aromatics could constitute a substantial portion of atmospheric organic N in aerosols collected in regions affected by biomass burning.

This study investigates the composition of organic particulate matter in a remote montane forest in the southeastern U.S., focusing on the role of organic N in sulfur-containing SOA and aerosols associated with biomass burning. Measurements target four groups of compounds: 1) nitro-aromatics associated with biomass burning; 2) organosulfates and nitrooxy-organosulfates produced from biogenic SOA precursors (i.e., isoprene, monoterpenes and unsaturated aldehydes) interacting with anthropogenic pollutants; 3) terpenoic acids formed from monoterpene oxidation; and 4) organic molecular markers including methyltetrols, C-5 alkene triols, 2-methylglyceric acid, 3-hydroxyglutaric acid and levoglucosan. Terpenoic acids and organic markers are included to assist in characterizing the extent of biogenic compound oxidation and atmospheric processing (i.e., aerosol aging) as well as contributions from biomass burning sources. Aerosol bulk chemical measurements are conducted to estimate total water soluble organic N and C concentrations. Characterization of seasonal patterns in concentrations of organic N species and assessment of potential sources and formation processes are emphasized.

2. Experimental methods and materials

2.1 Sampling site and atmospheric aerosol collection

The study was conducted at the U.S. Forest Service Coweeta Hydrologic Laboratory, a 2185-ha experimental forest in southwestern, North Carolina, USA (35°3' N, 83°25' W) near the southern end of the Appalachian Mountain chain. The climate is classified as maritime, humid temperate, with mean monthly temperatures ranging from 3.3ºC in January to 21.6ºC in July (Swift et al., 1988). Elevation ranges from 675 to 1592 m with a corresponding range in annual precipitation of 1800 to 2500 mm (Swank and Crossley, 1988). The vegetation is characterized as mixed coniferous/deciduous including oak, pines, and hardwoods (Bolstad et al, 1998). Atmospheric measurements were conducted in the lowest part of the basin (686 m), collocated with long term measurements of air and precipitation chemistry conducted by CASTNET and NADP networks, respectively.

The sampling site is 5 km west of Otto, NC (population 2500) and Highway 23 (Figure S1, supplemental material). Land to the north, west and south of Coweeta is undeveloped forest. Typical rural development is present to the east of the site, consisting of houses and small scale farming for hay and crop production including some scattered cow and horse pastures, which are small local ammonia (NH_3) emission sources. The nearest metropolitan areas include Atlanta, Georgia (175 km southwest), Chattanooga, Tennessee (175 km west), Knoxville, Tennessee (110 km north/northwest), Asheville, North Carolina (100 km northeast), and Greeneville, South Carolina (100 km southeast). The location of the sampling site within the context of NOx and SO_2 point sources in the eastern U.S. is shown in supplemental material (Figure S2). Only minor point sources are present within ~ 100 km of the site.

The study period summarized here comprises three seasonal intensives conducted during the spring, summer and fall of 2015 as part of the Southern Appalachia Nitrogen Deposition Study (SANDS). Each campaign was conducted for approximately 3 weeks (21 May to 9 June, 6 August to 25 August, 9 October to 26 October). A high-volume Tisch TE-1000 (Tisch Environmental, Cleves, OH) dual cyclone $PM_{2.5}$ sampler operated at a flow rate of 230 L/min was set up on the ground to collect 24 hr (started at 7am local time) integrated samples on pre-baked (550ºC for 12hrs) quartz fiber (QF) filters (90mm, Pall Corporation, Port Washington, NY). Under some conditions, the 24hr integrated filter sampling technique may not fully retain all semi-volatile organic nitrogen compounds (Gonzalez Benitez et al., 2009). Field blanks were collected the same way except being loaded in the sampler without the pump switched on. A total of 58 ambient samples and 10 field blanks were obtained. Collected filter samples were

transferred back to the laboratory in a cooler and stored in a freezer at -20 ºC before chemical analysis.

2.2 Trace gas and meteorological measurements

During the spring 2015 campaign, NOx concentrations were measured on a short tower (7 m above ground) co-located with the CASTNET and high volume PM samplers. NOx concentrations were measured using a commercial NO-NO_2-NOx analyzer (model 42S, Thermo Environmental Instruments, Incorporated, Franklin, MA). Briefly, nitric oxide (NO) is measured directly on one channel by chemiluminescence. On a 2nd channel, NO_2 is converted to NO by a molybdenum catalyst heated to 325ºC, yielding the concentration of NOx (NO + NO_2). This approach may overestimate NOx since other oxidized nitrogen gases such as HNO_3, PAN and HONO could also be reduced to NO on the heated molybdenum surface (Fehsenfeld et al., 1987; Williams et al.,1998; Zellweger et al., 2000). However, the use of an inlet filter and approximately 12 m of sample line between the atmospheric inlet and converter likely minimized the potential bias from HNO_3. For subsequent campaigns, NOx concentrations were estimated from a co-located NOy analyzer. Similar to the NOx instrument, NOy and HNO_3 were also measured using a modified model 42S NO-NO_2-NOx analyzer. The NOy technique is described in detail by Williams et al. (1998). Briefly, total oxidized reactive nitrogen (NOy) is converted to NO using a molybdenum catalyst heated to 325ºC. On a 2nd channel, a metal denuder coated with potassium chloride (KCl) is used to remove HNO_3 before passing through a 2nd molybdenum converter heated to 325ºC. The difference between the total NOy measurement and the HNO_3-scrubbed NOy measurement is interpreted as HNO_3. NOx concentrations were estimated from the differences between measured NOy and HNO_3, which provided an upper bound estimation as gaseous N containing species were not excluded (eg. PAN and organic nitrates). Hourly ozone concentrations were measured by CASTNET (U.S. EPA, 2017) on a co-located 10m tower. Hourly meteorological data were provided by CASTNET (U.S. EPA, 2017) and Forest Service (Miniat et al 2015; Oishi et al.,2017), including temperature, relative humidity, solar radiation and precipitation.

2.3 Chemical analysis

2.3.1 Elemental and organic carbon analysis

A 1.5cm^2 QF punch was analyzed for elemental carbon (EC) and organic carbon (OC) using a thermo-optical transmittance (TOT) method (Sunset Laboratory Inc, Oregon, USA) (Birch and Cary, 1996).

2.3.2 Water soluble species by Ion Chromatography (IC) and Total Organic Carbon/Total Nitrogen (TOC/TN) analyzers

A second QF punch (1.5cm^2) from each sample was extracted with DI water (18.2 MΩ·cm, Milli-Q Reference system, Millipore, Burlington, MA) in an ultrasonic bath for 45 min. The sample extract was filtered through a 0.2μm pore size PTFE membrane syringe filter (Iso-disc, Sigma Aldrich, St. Louis, MO) before subsequent analyses.

Water soluble organic carbon (WSOC) and total N (WSTN) concentrations were measured using a chemiluminescence method that included a total organic carbon analyzer (TOC-Vcsh) combined with a total nitrogen module (TNM-1) (Shimadzu Scientific Instruments, Columbia, MD). For WSOC measurements, 25% phosphoric acid was mixed with sample extract (resulting in a 1.5% acid mixture) and sparged for 3 min to remove any existing carbonate/bicarbonate.

Inorganic species (NH_4^+, NO_3^-, NO_2^- and SO_4^{2-}) were analyzed using ion chromatography (IC, Dionex model ICS-2100, Thermo Scientific, Waltham, MA). The IC was equipped with guard (IonPac 2mm AG23) and analytical columns (AS23) for anions. The samples were analyzed using an isocratic eluent mix carbonate/bicarbonate (4.5/0.8mM) at a flow rate of 0.25 mL/min. Cations were analyzed by Dionex IonPac 2mm CG12 guard and CS12 analytical columns; separations were conducted using 20mM methanesulfonic acid (MSA) as eluent at a flow rate of 0.25mL/min. Multi-point (≥5) calibration was conducted using a mixture prepared from individual inorganic standards (Inorganic Ventures, Christiansburg, VA). A mid-level accuracy check standard was prepared from certified standards mix (AccuStandard, New Haven, CT) for quality assurance/quality control purposes.

2.3.3 UV-Vis light absorption analysis

Several studies have shown that methanol can extract aerosol OC at higher efficiencies than water, and that a large fraction of light absorption in the near-UV and visible ranges is ascribed to water insoluble OC (Chen and Bond, 2010; Liu et al., 2013; Cheng et al., 2016). In this study, a QF punch (1.5 cm^2) was extracted with 5 mL methanol (HPLC grade, Thermo

Fisher Scientific Inc.) in a tightly closed amber vial, sonicated for 15 min, and then filtered through a 0.2 μm pore size PTFE filter (Iso-disc, Sigma Aldrich, St. Louis, MO). The light absorption of filtered extracts was measured with a UV-Vis spectrometer over λ = 200-900 nm at 0.2 nm resolution (V660, Jasco Incorporated, Easton MD). The wavelength accuracy is better than ± 0.3 nm; the wavelength repeatability is less than ± 0.05 nm. A reference cuvette containing methanol was used to account for solvent absorption. The UV-Vis absorption of field blank samples was negligible compared to ambient samples, but used for correction nonetheless. For ease of analysis, the absorption at 365 nm referencing to absorption at 700 nm was used as a general measure of the absorption by all aerosol chromophore components (Hecobian et al., 2010).

2.3.4. Analysis of isoprene and monoterpene SOA markers and anhydrosugars by GC-MS

Aliquots of each filter (roughly ¼) were extracted by 10 mL of methanol and methylene chloride mixture (1:1, v/v) ultrasonically twice (15 minutes each). The total extract was filtered and concentrated to a final volume of ~0.5 mL. Next, extracts were transferred to a 2 mL glass vial and concentrated to dryness under a gentle stream of ultrapure N_2 and reacted with 50 μL of N, O-bis(trimethylsilyl)trifluoroacetamide (BSTFA) containing 1% trimethylchlorosilane (TMCS) and 10 μL of pyridine for 3 h at 70 °C. After cooling down to room temperature, internal standards (mixture of 17.6 ng μL^{-1} acenaphthalene-d10 and 18.6 ng μL^{-1} pyrene-d4 mixed in hexane) and pure hexane were added. The resulting solution was analyzed by an Agilent 6890N gas chromatograph (GC) coupled with an Agilent 5975 mass spectrometer (MS) operated in the electron ionization mode (70 eV). An aliquot of 2 μL of each sample was injected in splitless mode. The GC separation was carried out on a DB-5 ms capillary column (30 m × 0.25 mm × 0.25 μm, Agilent Technologies, Santa Clara, CA). The GC oven temperature was programmed from 50 °C (hold for 2 min) to 120 °C at 30 °C min^{-1} then ramped at 6 °C min^{-1} to a final temperature of 300 °C (hold for 10 min). Linear calibration curves were derived from six dilutions of quantification standards. Anhydrosugars (levoglucosan) were quantified using authentic standard; 2-methyltetrols (2-methylthreitol and 2-methylerythritol) and C-5 alkene triols were quantified using meso-erythritol; other SOA tracers (e.g., hydroxyl dicarboxylic acid) were quantified using cis-ketopinic acid (KPA) (refer to supplemental information Table S1). The species not quantified using authentic standards were identified by the comparison of mass

spectra to previously reported data (Claeys, et al., 2004, 2007; Surratt et al., 2006; Kleindienst et al., 2007). Field blanks were collected and no contamination was observed for identified species.

2.3.5. Analysis of organosulfates, terpenoic acids and nitro-aromatics by High Performance Liquid Chromatography- electrospray ionization-Quadrupole time-of-flight-Mass Spectrometer (HPLC-ESI(-)-QTOF-MS)

Approximately 3-5 mL of methanol was used to ultrasonically extract (twice for 15 min) roughly half of each 90mm QF sample. Internal standards (I.S.) were spiked onto each filter sample prior to extraction (refer to Table S2, S3 and S4 for individual compounds and surrogate standards used for each group of compounds). Extracts were filtered into a pear-shaped glass flask (50 mL) and rotary evaporated to ~0.1 mL. The concentrated extracts were then transferred into a 2 mL amber vial that was rinsed with methanol 2-3 times. The final sample extract volume was ~500 μL prior to analysis. All the glassware used during the extraction procedure was pre-baked at 550°C overnight. Extracted samples were stored at or below -20 °C prior to analysis and typically analyzed within 7 d.

An HPLC coupled with a quadrupole time-of-flight mass spectrometer (1200 series LC and QTOF-MS, Model 6520, Agilent Technologies, Palo Alto, CA) was used for target compound identification and quantification. The QTOF-MS instrument was equipped with a multimode ion source operated in electrospray ionization (ESI) negative (-) mode. Optimal conditions were achieved under parameters of 2000 V capillary voltage, 140 V fragmentor voltage, 65 V skimmer voltage, 300 °C gas temperature, 5 L/min drying gas flow rate and 40 psig nebulizer. The ESI-QTOF-MS was operated over the m/z range of 40 to 1000 at a 3 spectra/s acquisition rate. Target compounds separation was achieved by a C18 column (2.1×100 mm, 1.8 μm particle size, Zorbax Eclipse Plus, Agilent Technologies) with an injection volume of 2 μL and flow rate of 0.2 mL/min. The column temperature was kept at 40 °C, and gradient separation was conducted with 0.2% acetic acid (v:v) in water (eluent A) and methanol (eluent B). The eluent B was maintained at 25% for the first 3 min, increased to 100% in 10 min, held at 100% from 10 to 32 min, and then dropped back to 25% from 32 to 37 min, with a 3 min post run time. During each sample run, reference ions were continuously monitored to provide accurate mass corrections (purine and HP-0921 acetate adduct, Agilent G1969-85001). Typically, the instrument exhibited 2 ppm mass accuracy. Tandem MS was conducted by

targeting ions under collision-induced dissociation (CID) to determine parent ion structures. Agilent software Mass hunter was used for data acquisition (Version B05) and for further data analysis (Qualitative and Quantitative Analysis, Version B07). The mass accuracy for compound identification and quantification was set at ± 10 ppm. Calibration curves were generated from diluted standard compound mixtures. Recoveries of the extraction and quantification were performed by spiking known amounts of standards to blank QF filters. Then the spiked blank filters were extracted and analyzed the same way as ambient collected samples. The average recoveries of standard compounds are listed in supplemental information Table S5 and ranged from 75.2 ± 5.6 to 129.4±4.2%. Isomers were identified for several compounds, no further separation was conducted and combined total concentrations are reported in this study.

2.4 Source apportionment by Positive Matrix Factorization

Positive Matrix Factorization (PMF) was used to identify potential sources of compounds measured at Coweeta. Here we use the PMF2 model (Paatero, 1998a, b) coupled with a bootstrap technique (Hemann et al., 2009), which has been applied in a number of previous studies (Xie et al., 2012, 2013, 2014,). Briefly, PMF resolves factor profiles and contributions from a series of PM compositional data with an uncertainty-weighted least-squares fitting approach; the coupled stationary bootstrap technique generates 1000 replicated data sets from the original data set and each was analyzed with PMF. Normalized factor profiles were compared between the base case solution and bootstrapped solutions, so as to generate a factor matching rate. The determination of the factor number was based on the interpretability of different PMF solutions (3-6 factors) and factor matching rate (>50%). Detailed data selection criteria are presented in supplemental information.

3. Results and discussion

3.1 Meteorology, NOx, and O_3

Statistics of atmospheric chemistry and meteorological measurements are summarized by season in Table 1. In general, the sampling site was humid and cool, even in the summer, with an average summer temperature of ~21ºC and RH of 82%. During the fall, much lower temperature (~12 ºC) and less humid conditions (RH=78%) were observed. NOx concentrations

were generally less than 1ppb, which is considered typical for such a remote forest site removed from major emission sources.

[O_3] (O_3 concentration) was generally low (Table 1) with seasonal averages of 15 ppb to 25 ppb. Historical seasonal [O_3] over the past 5 years (2011 to 2015) are shown in supplemental information Figure S3. A spring maximum in [O_3] is typically observed at this site, with lower concentrations during summer. Seasonal clustered back trajectories (Figure S4 in supplemental information) suggest that during spring the Coweeta sampling site was under the influence from air masses transported from Atlanta urban areas. In addition, a spring maximum [O_3] may be due to higher chemical consumption of O_3 by reactive monoterpenes and sesquiterpenes emitted in the forest during summer. With observed relatively moderate summer temperatures and generally low [NOx], the site also experiences frequent cloud cover in summer lowering the intensity of solar radiation which may suppress ozone production relative to spring conditions. Additionally, deposition of O_3 to the forest would be expected to peak during the summer, when leaf area is greatest. O_3 correlates positively with NOx in summer and fall but not spring, indicating O_3 production might be relatively more VOC-limited in spring than the other seasons in this region.

3.2 Bulk water soluble organic nitrogen and carbon

Water soluble bulk organic N (WSON) was estimated as the difference between WSTN and the sum of the inorganic N species (NH_4^+, NO_3^- and NO_2^-). The measurement uncertainty of WSON was estimated to be ~30% from error propagation of WSTN (2%), NH_4^+ (1%), NO_3^- (1%) and NO_2^- (1%). Nitrogen component contributions to WSTN are presented in Figure 1a, which shows NH_4^+ as the most abundant component, contributing 85±11% w/w to total WSTN mass. Typical NH_4^+ concentrations at the site were below 1.0 μg/m^3(with an average of 0.32 μg/m^3), which is expected for such a remote site with no major local or regional NH_3 sources. The oxidized inorganic N components (NO_3^- and NO_2^-) accounted for less than 2% w/w of WSTN measured. Such a small contribution of NO_3^- to inorganic N (typically <10% of inorganic N (NO_3^-+NH_4^+)) in $PM_{2.5}$ is consistent with long term CASTNET measurements at Coweeta. The average contribution of WSON to WSTN over the entire study period was 14±11% w/w. This fraction reached a maximum of ~18% w/w in the spring (average) and minimum of ~10% in the fall (average), exhibiting pronounced seasonal variability. Within individual samples (Figure 1b),

values ranged from near zero to 45%. Our study wide average of 14% falls within the range of measurements at North American forest sites, including Duke Forest, North Carolina (~33%, Lin et al., 2010) and Rocky Mountain National Park (14-21%) (Benedict et al., 2012). Moreover, the observed WSON contribution to WSTN in particles at Coweeta is consistent with a global estimated range of 10-39% (Cape et al., 2011).

WSOC accounted for roughly 62±13% of OC throughout the entire study period with no significant seasonal variability. A time series of OC and WSOC along with temperature and precipitation is presented in Figure 1c. On average, OC concentrations increased during warmer spring and summer seasons and decreased when the temperature decreased in fall. Concentrations of OC were positively correlated with temperature ($r=0.30$, $p<0.05$), presumably in response to emissions of biogenic precursors and formation of secondary organic aerosols by photooxidation. Spring and summer were generally moist and warm with frequent precipitation (relative humidity presented in Table 1). Precipitation events corresponded to decreasing OC and WSOC concentrations demonstrating the scavenging effect due to wet deposition.

Spearman rank correlation coefficients among measured species and meteorological variables as well as other gas phase measurements are presented in Table 2 for each season ($p<0.01$ for values in bold). As expected, NH_4^+ and SO_4^{2-} tracked well over each season ($r>0.9$, $p<0.01$). NH_4^+ was mainly associated with SO_4^{2-} given the fact that NO_3^- and NO_2^- were generally negligible compared to SO_4^{2-}. WSOC is often used as an SOA surrogate and accounts for a significant portion (62% w/w) of OC during all sampling periods. WSOC correlated strongly with OC over both summer and fall ($r>0.95$, $p<0.01$), but less so during spring ($r=0.74$, $p<0.01$). WSOC also positively correlates with WSON over spring and fall ($r>0.75$, $p<0.01$) but less so during summer ($r = 0.5$, $p > 0.01$). Note that both [WSOC] and [OC] are highest in the summer, which likely indicates higher biogenic emissions and SOA formation. However, the weak WSON-WSOC correlation suggests a variety of source contributions to WSON and WSOC over the different seasons. [EC] was negligible over the entire study except a modest spike at the end of October when wood burning was most likely the source. Details of this event are discussed in the subsequent sections. It is also noted that a stronger correlation of WSON with NH_4^+ than with NO_3^- was observed, which might suggest a key role of reduced nitrogen in WSON formation (Cape et al., 2011; Jickells et al., 2013).

3.3 Nitro-aromatics

Concentrations of nitro-aromatics, organosulfate/nitrooxy-organosulfate, and terpenoic acids are summarized in Tables 3, S2, S3 and S4. A time series of compound class totals are presented in Figure 2. Generally negligible concentrations of nitro-aromatics were observed during spring and summer except for occasional spikes. However, higher concentrations of nitro-aromatics were observed in the fall when moderate correlations were observed with levoglucosan (Figure 3, $r \geq 0.5$, $p < 0.01$; see table SI 6 for correlation coefficients). A residential wood burning contribution is likely given the lower temperatures observed during this season. Similar positive correlations between nitro-aromatics and wood burning are also reported during the winter season (Gaston et al., 2016; Kahnt et al., 2013; Kitanovski et al., 2012; Iinuma et al., 2010, 2016). Smoke at the sampling site on October 19th and 21st coincided with firewood burning at the main office of the Coweeta Hydrologic Laboratory, immediately adjacent to the sampling location. Nitro-aromatics were relatively elevated, but no significant increase in organosulfates or terpenoic acids were found from these fresh smoke events. In contrast, an example of an aged biomass burning signal is illustrated on October 24th and 25th. Pronounced spikes of nitrocatechol($C_6H_5NO_4$), methyl-nitrocatechol($C_7H_7NO_4$) and levoglucosan were observed (Figure 3), along with elevated concentrations of organosulfates, OC and aged biogenic aerosol tracers (terpenoic acids m/z 203 and 187 shown in Figure 4a, detailed discussion can be found in the subsequent section). However, EC was only slightly higher. This event did not correspond to local burning at Coweeta and was most likely associated with long range transport. Clustering of backward trajectories (120hr duration for individual trajectories; 48 total trajectories covering the two-day event) suggests that northeast Georgia (shown in supplemental information Figure S5) is the most likely origin of the biomass burning event observed on October 24th and 25th.

Nitro-aromatics correlate with EC across the seasons; both are likely emitted from biomass burning (Gaston et al., 2016; Iinuma et al., 2010; Kahnt et al., 2013; Mohr et al., 2013). Interestingly, light absorption at λ= 365nm is highly correlated ($r=0.80$, $p<0.01$) with nitro-aromatics in the fall when nitro-aromatic concentrations were elevated. In addition, NOx correlates inversely ($r=-0.72$, $p<0.01$) with temperature in the fall. Lower fall temperatures in the region may have resulted in frequent residential wood burning, which emits NOx and light absorbing BrC (eg. nitro-aromatics) (Liu et al., 2015; Mohr et al., 2013). Although nitro-

aromatics account for a minor fraction of OM, they could potentially contribute to 4% of light absorption by BrC (Mohr et al., 2013). Overall, nitro-aromatics displayed relatively week correlation with WSON ($r<0.65$) across all seasons; the extremely low concentrations observed suggest a generally small contribution of nitro-aromatics to WSON at the sampling site, hence the lack of strong correlation.

3.4 Organosulfates and nitrooxy-organosulfates

Organosulfate concentrations were highest in summer and lowest in fall (Table 3), contributing 3.9 and 1.0 % w/w of organic matter (OM, estimated by applying an OM/OC factor of 2) mass, respectively, during these seasons. Organosulfate formation is an example of heterogeneous chemistry involving uptake of reactive precursors on acidified sulfate aerosols requiring a mixture of biogenic and anthropogenic emissions. The air masses at Coweeta are mainly from the southwest and westerly directions in spring and summer, but during fall may become more stagnant and slow moving during southwesterly conditions or shift to the northwest (see clustered back trajectories are shown in Figure S4). Because Atlanta, GA is southwest of Coweeta, southwesterly flow during spring and summer may be associated with long range transport of urban pollutants and precursors, including sulfate and sulfuric acid, leading to elevated organosulfate formation compared to fall when the prevailing wind direction changes.

Among all organosulfates identified, the isoprene derived organosulfate (m/z 215, 2-methyltetrol derived), which is formed from isoprene derived epoxydiols (IEPOX) under low NOx conditions, was the most abundant; concentrations reached 167 ng/m^3 in summer. Similar high concentrations were also reported in ambient samples collected at other sites in the southeastern U.S. (Lin et al., 2013b; Worton et al., 2013). Of the six nitrooxy-organosulfates identified, isoprene derived m/z 260 was most abundant, approximately 6-fold higher than monoterpene derived m/z 294 nitrooxy-organosulfate.

A subset of possible organosulfates and nitrooxy-organosulfates produced from isoprene and monoterpene oxidation exhibit strong correlations with distinctive SOA tracers (eg. markers 2-methylglyceric acid, C-5 alkene triols and methyltetrols for isoprene oxidation products; tracer 3-Hydroxyglutaric acid for pinene oxidation products) (see table SI 7). Lack of correlation between nitrooxy-organosulfate m/z 294 and 3-hydroxyglutaric acid may indicate a favored nighttime nitrate radical formation pathway over photochemical oxidation. Given that NOx

levels at the rural Coweeta sampling site were typically less than 1ppb, photo-oxidation pathways involving high [NOx] to form nitrooxy-organosulfates are less likely. Though a contribution from photochemical oxidation cannot be ruled out (Lee et al., 2016; Romer et al., 2016), nighttime nitrate radical chemistry is most likely the dominating formation mechanism under such conditions. In contrast to our observations, He et al. (2014) report good correlations ($r>0.5$, $p<0.01$) of m/z 294 with 3-hydroxygluraric acid and higher daytime m/z 294 concentrations for summer samples collected in Pearl River Delta, China, where a seasonal average NOx level of 30 ppb was observed. The authors suggested that the dominant m/z 294 formation pathway was through daytime photochemistry rather than nighttime NO_3 chemistry. The extremely low NOx levels at our study site compared to that measured by He et al. may explain the opposite behavior in terms of m/z 294 formation mechanisms.

Organosulfates exhibited statistically significant correlations with WSON only in the summer ($r=0.64$, $p<0.01$), which reflected the importance of N containing organosulfates or their formation chemistry to WSON during summer compared to the other seasons. During this season, nitrooxy-organosulfates accounted for ~2% of bulk WSON, on average. A strong correlation may therefore not be expected.

3.5 Terpenoic acids

Terpenoic acids, which provide insight into the extent of biogenic compound oxidation and atmospheric processing (i.e., aerosol aging), were the most abundant group of compounds relative to nitro-aromatics and organosulfates. On average, terpenoic acids accounted for 6.5 to 8.7% w/w of OM in $PM_{2.5}$. The warmer spring and summer periods show higher production of terpenoic acids compared to the cool and drier fall season. Higher emissions of biogenic VOC precursors as well as higher solar radiation intensities during warm seasons, which drive photochemistry, are factors contributing to observed seasonal variability.

The terpenoic acids correlate well with WSOC and OC (Table 2). This is expected as terpenoic acids account for a substantial portion of OM at the site. Individual acids (except compounds $C_7H_{10}O_4$ and $C_9H_{14}O_4$) exhibit strong correlations with the pinene derived SOA tracer 3-hydroxyglutaric acid ($r>0.75$, $p<0.01$; correlation coefficients shown in the supplemental information Table S8), indicating the presence of α-/β-pinene oxidation products. The poor correlations between acids $C_7H_{10}O_4$ (m/z 157) and $C_9H_{14}O_4$ (m/z 185) suggests the presence of

biogenic VOC precursors other than α-/β-pinene, such as limonene and Δ^3-carene (Gomez-Gonzalez et al., 2012).

Recent chamber studies identified several terpenioc acid structures also observed in ambient aerosol samples, including 3-methyl-1,2,3-butanetricarboxylic acid (MBTCA, $C_8H_{12}O_6$, m/z 203), 2-hydroxyterpenylic acid ($C_8H_{12}O_5$, m/z 187), terpenylic acid ($C_8H_{12}O_4$, m/z 171) and diaterpenylic acid acetate (DTAA, $C_{10}H_{16}O_6$, m/z 231) (Claeys et al., 2009; Kahnt et al., 2014). MBTCA and 2- hydroxyterpenylic acid have been identified as highly oxygenated, higher generation α-pinene SOA markers, and observed in high abundance in ambient aerosols (Gomez-Gonzalez et al., 2012; Kahnt et al., 2014; Muller et al., 2012; Szmigielski et al., 2007). Additionally, terpenylic acid and DTAA are characterized as early photooxidation products from α-pinene ozonolysis. Claeys et al. (2009) proposed further oxidation processes (aging) of terpenylic acid involving OH radical chemistry to form 2- hydroxyterpenylic acid. Figure 4 provides a time series of the terpenoic acids identified in this study. In general, 2-hydroxyterpenylic acid was the most abundant species across the seasons. To assess the extent of aging, concentration ratios of higher generation oxidation products ($C_8H_{12}O_6$, m/z 203 and $C_8H_{12}O_5$, m/z 187) to early oxidation fresh SOA products ($C_8H_{12}O_4$, m/z 171 and $C_{10}H_{16}O_6$, m/z 231) are calculated. Estimated seasonal averages of these ratios are 3.98, 4.37 and 2.44 for spring, summer and fall, respectively. Thus, during spring and summer, aerosols observed at the site were more aged. Figure 4 shows the correlation of these ratios with temperature ($r=0.79$, $p<0.001$) and solar radiation ($r=0.23$, $p<0.1$). A clear relationship between temperature and OH radical initiated oxidation (aging) is evident. However, oxidation appears less dependent on solar radiation at our sampling site. Similar higher contribution of these aged biogenic SOA tracers was also reported under warm summer conditions characterized by high temperature and high solar radiation (Claeys et al., 2012; Gomez-Gonzalez et al., 2012; Hamilton et al., 2013; Kahnt et al., 2014). Based on the typical chemical lifetime of biogenic SOA by OH oxidation and the precipitation frequency at Coweeta site, biogenic SOA collected at Coweeta probably had an atmospheric lifetime of several days before depletion by oxidation processes and/or scavenging by precipitation (Epstein et al., 2014).

Terpenoic acids may also provide some insight into the formation mechanisms of organosulfates. While organosulfate concentrations are highest during summer, correlations with SO_4^{2-} are strongest during spring and fall and weakest during summer. Conversely,

organosulfates and terpenoic acids correlate strongly (r=0.91. p<0.01) during summer. Terpenoic acids are either first or second generation oxidation products from gas phase monoterpenes; particulate SO_4^{2-} abundance should not substantially influence the gas-particle partitioning of terpenoic acids. The strong correlation between organosulfates and terpenoic acids in summer suggests organosulfate formation is limited by monoterpene emissions rather than SO_4^{2-} availability while in the spring and fall (especially fall), organosulfate production may be more limited by SO_4^{2-}. Degree of particle neutralization, calculated as the molar ratio of NH_4^+ to the sum of $SO_4^{2-}$and NO_3^-, averaged 0.94, 0.98 and 0.94 for spring, summer and fall, respectively. Neutralization being close to but less than unity implies that aerosols are slightly acidic at the site. Chamber studies have illustrated that acidified SO_4^{2-} could enhance heterogeneous reactions to form SOA from isoprene and monoterpenes (Iinuma et al., 2009; Surratt et al., 2007, 2010). Similar positive correlations observed at the Coweeta site were also found between isoprene tracers including isoprene derived organosulfates and SO_4^{2-} by Lin et al. (2013b) at a rural site in the southeastern U.S. However, in contrast to chamber experiments, this study and other ambient field measurements have not provided clear evidence of acidity enhancement of organosulfate formation (He et al., 2014; Lin et al., 2013b; Worton et al., 2011), indicating possible differences in exact mechanisms and processing to form these organosulfates under atmospheric conditions relative to chamber studies. Recent mechanistic modeling simulations by Budisulistiorini et al., (2017) suggest that the role of sulfate on IEPOX-organosulfates formation might be through surface area uptake of IEPOX and rate of particle phase reaction.

Very good correlations between WSON and terpenoic acids were observed during summer and fall ($r \geq 0.7$, $p < 0.01$). Given the secondary nature of terpenoic acids, this finding may suggest that WSON during these two seasons is associated with more aged air masses and perhaps dominated by secondary organic components rather than primary emitted N containing constituents such as pollens, fungi and bacteria (Elbert et al., 2007; Miyazaki et al., 2014).

3.6 Contribution of identified N containing species to WSTN and WSON

Nitro-aromatics and nitrooxy-organosulfates combined were estimated to account for as much as 28% of WSON for samples impacted by local biomass burning, which reflected the abundance and potential importance of these groups of species to the atmospheric N deposition budget. Seasonal average ratios of identified WSON to WSTN ranged from 1.0 to 4.4% with the

highest recorded for fall (Table 4). Nitrooxy-organosulfates dominated over nitro-aromatics as a source of organic nitrogen, contributing > 90% to identified WSON across seasons. However, during episodes of biomass burning, nitro-aromatics contribute as much as 32% of identified WSON compounds. The ratio of WSON to WSOC was estimated to be 0.05, 0.04 and 0.02 for spring, summer and fall, which implies organic N being most enriched during spring, reflecting a spring maximum in seasonal emissions of organic N from biological sources (e.g. pollens, spores, leave litter decomposition) combined with smaller contributions from secondary atmospheric processes. The observed WSON/WSOC ratios in this study were slightly lower than those reported for other forest sites (0.03-0.09) (Lin et al., 2010; Miyazaki et al., 2014), which are not as remote and pristine as the forest site in this study. Anthropogenic influences at the study sites described by Lin et al. (2010) and Miyazaki et al. (2014) such as [SO_4^{2-}] and [NOx] were ~ 5 times higher than those measured at the Coweeta site. Concentration weighted average WSON/WSOC ratios for identified compounds (nitro-aromatics, organosulfates/nitrooxy-organosulfates and terpenoic acids) in this study were estimated to be 0.003. This value is 10 times less than the overall WSON/WSOC ratio observed at the site, which indicates existence of other higher N content species in the aerosols. Moreover, the identified ON/WSON percentage was estimated to be 1.0, 2.0 and 4.4 for spring, summer and fall, respectively. Such differences further suggest much more unidentified WSON compounds exist in spring when organic N was most enriched from biological processes.

3.7 PMF analysis

PMF analysis was conducted to identify individual source contributions to total WSOC. Factor profiles and time series of factor contributions are presented in figures 5 and 6. Listed in order of percent contribution to WSOC, the five factors which were resolved include secondary sulfate processing (35.3%), isoprene SOA (24.3%), WSON containing OM (20.0%), biomass burning (15.1%) and monoterpene SOA (5.2%). Overall, these factors could explain 89±2% of observed WSOC ($r=0.88$, $p<0.0001$). The secondary sulfate profile contained a signature of high SO_4^{2-}, which was most likely present as fine particulate $(NH_4)_2SO_4$ and NH_4HSO_4. Secondary sulfate was the most important factor during spring, though was a significant contributor in summer and fall as well. Isoprene SOA, which was identified based on isoprene derived organosulfates and isoprene SOA markers, was the most important factor during summer. The

biomass burning factor, which exhibited a high portion of nitro-aromatic and levoglucosan markers, dominated in the fall. This pattern agreed well with observed patterns of nitro-aromatic compounds. Monoterpene SOA, which was resolved based on the composition of monoterpene derived organosulfates, was overall a minor contributor with the exception of a few samples during the fall intensive.

WSON containing OM contributed 20% to WSOC, overall, demonstrating a significant association between organic N and C in $PM_{2.5}$ at our study site. The WSON containing OM source profile exhibited weak correlation with most measured species with the exception of modest correlations with terpenoic acids. WSON containing OM contributed more to WSOC in late spring and early summer, which was consistent with observed higher production of nitrooxy-organosulfates during these sampling periods as well as terpenoic acids. The relationship with terpenoic acids may reflect an association of WSON with more aged air masses. Because nitro-aromatics and nitrooxy-organosulfates contribute only a small portion of WSON, on average, the 20% contribution of WSON containing OM to WSOC primarily reflects the contribution of organic N present in bulk WSON but unspeciated in this work.

4. **Conclusions**

Ambient $PM_{2.5}$ collected at a temperate mountainous forest site were investigated on a bulk chemical and a molecular level during spring, summer, and fall of 2015. Analyses focused on speciation of nitro-aromatics associated with biomass burning, organosulfates produced from biogenic SOA precursors, and terpenoic acids formed from monoterpene oxidation. Among these three groups, terpenoic acids were estimated to be most abundant, contributing up to a seasonal average of 8.7% of OM in $PM_{2.5}$ during spring. Warm periods in spring and summer exhibited highest production of terpenoic acids, when SOA correspondingly showed a higher degree of aging. Relative abundance of aged biogenic SOA tracers (MBTCA and 2- hydroxyterpenylic acid), which reflect the degree of organic aerosol aging, showed a strong correlation with temperature. Such a relationship might indicate temperature dependence of OH radical initiated oxidation steps or aging in the formation of higher generation oxidation products.

Organosulfates showed a peak in summer and lowest concentrations during fall, contributing averages of 3.9 and 1.0 % of OM mass, respectively, during these seasons. Isoprene derived organosulfate (m/z 215, 2-methyltetrol derived), formed from isoprene derived

epoxydiols (IEPOX) under low NOx conditions, was the most abundant identified organosulfate (up to 167 ng/m^3 in summer). This observation is consistent with observations of low NOx levels (< 1ppb on average) at our study site. Nighttime nitrate radical chemistry is most likely the dominant formation mechanism for nitrooxy-organosulfates measured at this remote site with background level NOx.

Nitro-aromatics were most abundant at our study site during the fall (up to 0.01% of OM mass). Moderate correlations were observed between nitro-aromatics and the biomass burning marker levoglucosan, indicating a common origin. Nitro-aromatics also correlated well with EC across seasons. Highest concentrations of nitro-aromatics, specifically nitrocatechol and methyl-nitrocatechol, were associated with aged biomass burning plumes as indicated by correspondingly high concentrations of terpenoic acids.

Bulk measurements determined that WSOC accounted for 62±13% of OC throughout the entire study period without significant seasonal variability. PMF analysis indicated that a significant portion of this organic carbon was associated with a resolved factor of WSON containing OM. As a component of total nitrogen in $PM_{2.5}$, largest contributions of WSON to WSTN were observed in spring (~ 18% w/w) and lowest in the fall (~10% w/w). On average, identified nitro-aromatic and nitrooxy-organosulfate compounds accounted for a small fraction of WSON, ranging from ~ 1% in spring to ~ 4% in fall, though were observed to contribute as much as 28% w/w of WSON in individual samples which were impacted by local biomass burning. Of the organic N compounds speciated in this study, nitrooxy-organosulfates dominated over nitro-aromatics as a source of organic nitrogen, contributing > 90% to WSON across seasons. As a component of WSON, nitro-aromatics were most important during episodes of biomass burning, when their contribution to identified and total WSON was as much as 32% and 3%, respectively. Concentration weighted average WSON/WSOC ratios for compounds identified in this study were estimated to be 0.003. This number is an order of magnitude lower than the overall WSON/WSOC ratio observed, indicating a predominance of other uncharacterized N species. Other N containing substituents of WSON could include amino acids, amines, urea and N-heterocyclic compounds as well as substances of biological origin such as spores, pollens and bacteria (Cape et al., 2011; Neff et al., 2002a). Ratios of WSON to WSOC indicate organic C being most enriched by organic N during spring, perhaps reflecting a

623 spring maximum in seasonal emissions of organic N from biological sources combined with
624 smaller contributions from secondary atmospheric processes (e.g., nitrooxy-organosulfates).
625 Although nitro-aromatics and nitrooxy-organosulfates contribute a relatively small
626 fraction of organic N in $PM_{2.5}$ at our study site, our observations shed light on this complex but
627 largely unknown portion of the atmospheric N budget. Our results provide further understanding
628 of the patterns and composition of SOA in a remote mountain environment previously
629 uncharacterized. Similar to our results, other studies generally find that individual groups of
630 organic N compounds (e.g., amines, amino acids, urea) cannot explain the majority of bulk
631 WSON, (Cape et al., 2011; Day et al., 2010; Place et al., 2017; Samy et al., 2013), which
632 globally accounts for ~25% of total N in rainfall (Cape et al., 2011; Jickells et al., 2013). As
633 methodological advances allow for greater speciation of this large pool of atmospheric N, future
634 work should emphasize analysis of both primary and secondary forms of organic N in individual
635 samples, in addition to bulk analyses, so that a more complete picture of organic N composition
636 may be developed for specific atmospheric chemical and meteorological conditions.
637 Additionally, as progress is made in better characterizing the composition and sources of
638 atmospheric organic N, the ecological and atmospheric science communities must work together
639 to develop a better understanding of the role of atmospheric organic N in ecosystem N cycling.
640

641 **Supplemental Information available**

642

643 **Acknowledgements**

644

645 We would like to acknowledge Pamela Barfield, Ryan Daly, Aleksandra Djurkovic, David
646 Kirchgessner, John Offenberg, Bakul Patel and Bill Preston for laboratory and field support. We
647 also would like to thank Joshua G. Hemann and Michael P.Hannigan for the PMF source codes
648 and Christopher Oishi, Patsy Clinton and Chuck Marshall for assistance with meteorological data
649 sets. We would like to thank the U.S. Forest Service, Southern Research Station for the
650 opportunity to conduct this study at the Coweeta Hydrologic Laboratory and for the contribution
651 of meteorological data used in our analysis. We also thank internal EPA reviewers Chris Geron
652 and Havala Pye for their comments and suggestions. The views expressed in this article are those
653 of the authors and do not necessarily represent the views or policies of the U.S. EPA. Mention
654 of trade names does not constitute endorsement or recommendation of a commercial product by
655 U.S. EPA.

656

References

Altieri, K.E., Turpin, B.J., and Seitzinger S.P., 2009. Composition of dissolved organic nitrogen in continental precipitation investigated by Ultra-High Resolution FT-ICR Mass Spectrometry. Environmental Science and Technology 43, 6950-6955.

Altieri, K.E., Hastings, M.G., Peters, A.J., Sigman, D.M., 2012. Molecular characterization of water soluble organic nitrogen in marine rainwater by ultra-high resoluation electrospray ionization mass spectrometry. Atmospheric Chemistry and Physics 12. 3557-3571.

Benedict, K.B., 2012. Observations of atmospheric reactive nitrogen species and nitrogen deposition in the Rocky Mountains. Dissertation, Colorado State University. https://dspace.library.colostate.edu/handle/10217/71545

Birch, M. E. and Cary, R. A.: Elemental carbon-based method for monitoring occupational exposures to particulate diesel exhaust, Aerosol Science and Technology, 25, 221–241, 1996.

Bobbink, R., Hornung M., and Roelofs, J.M., 1998. The effects of air-borne nitrogen pollutants on species diversity in natural and semi-natural European vegetation. Journal of Ecology 86, 717-738.

Bolstad, P.V., Swank, W., Vose, J., 1998. Predicting Southern Appalachian overstory vegetation with digital terrain data. Landscape Ecology 13, 271-283.

Bragazza, L., Freeman, C., Jones, T., Rydin, H., Limpens, J., Fenner, N., Ellis, T., Gerdol, R., Hajek, M., Iacumin, P., Kutnar, L., Tahvanainen, T., and Toberman, H., 2006. Atmospheric nitrogen deposition promotes carbon loss from peat bogs. Proceedings of the national academy of Science 103, 19386-19389.

Budisulistiorini, S.H., Nenes, A., Carlton, A.G., Surratt, J.D.,,McNeill, V.F., Pye, H.O.T., 2017. Simulating aqueous-phase isoprene-epoxydiol(IEPOX) secondary organic aerosol production during the 2013 Southern Oxidation and Aerosol Study(SOAS). Environmental Science and Technology 51, 5026-5034.

Cape, J.N., Cornell, S.E., Jickells, T.D., Nemitz, E., 2011. Organic nitrogen in the atmosphere-Where does it come from? A review of sources and methods. Atmospheric Research 102, 30-48.

Chan, M.N., Surratt, J.D., Claeys, M., Edgerton, E.S., Tanner, R.L., Shaw, S.L., Zheng, M., Knipping, E.M., Eddingsaas, N.C., Wennberg, P.O., Seinfeld, J.H., 2010. Characterization and quantification of isoprene-derived epoxydiols in ambient aerosol in the Southeastern United States. Environmental Science and Technology 44, 4590-4596.

Chen, Y., Bond, T.C., 2010. Light absorption by organic carbon from wood combustion. Atmospheric Chemistry and Physics 10, 1773-1787.

Cheng, Y., He, K.-b., Du, Z.-y., Engling, G., Liu, J.-m., Ma, Y.-l., Zheng, M., Weber, R.J., 2016. The characteristics of brown carbon aerosol during winter in Beijing. Atmospheric Environment 127, 355-364.

Claeys, M., Graham, B., Vas, G., Wang, W., Vermeylen, R., Pashynska, V., Cafmeyer, J., Guypn, P., Andreae, M.O., Artaxo, P., Maenhaut, W., 2004. Formation of secondary organic aerosols through photooxidation of isoprene. Science 303, 1173-1176.

Claeys, M. Szmigielski, R., Kourtchev, I., Van Der Veken, P., Vermeylen., R., Maenhaut, W., Jaoui, M., Kleindienst, T.E., Lewandowski, M., Offenberg, J.H., Edney, E.O., 2007. Hydroxydicarboxylic acids: Markers for secondary organic aerosol from the photooxidation of α-pinene. Environmental Science and Technology 41, 1628-1634.

Claeys, M., Iinuma, Y., Szmigielski, R., Surratt, J.D., Blockhuys, F., Van Alsenoy, C., Boge, O., Sierau, B., Gomez-Gonzalez, Y., Vermeylen, R., Van Der Veken, P., Shahgholi, M., Chan, A.W.H., Herrmann, H., Seinfeld, J.H., Maenhaut, W., 2009. Terpenylic acid and related compounds from the oxidation of α-pinene: Implications for new particle formation and growth above forests. Environmental Science and Technology 43, 6976-6982.

Claeys, M.; Vermeylen, R.; Yasmeen, F.; Gómez-González, Y.; Chi, X. G.; Maenhaut, W.; Mészáros, T.; Salma, I.,2012. Chemical characterisation of humic-like substances from urban, rural and tropical biomass burning environments using liquid chromatography with UV/vis photodiode array detection and electrospray ionization mass spectrometry. Environmental Chemistry 9, 273−284.

Darer, A.I., Cole-Filipiak, N.C., O'Connor, A.E., Elrod, M.J., 2011. Formation and stability of atmospherically relevant isoprene-derived organosulfates and organonitrates. Environmental Science and Technology 45, 1895-1902.

Day, D. A., Liu,S., Russell, L. M. and Ziemann, P. J., 2010. Organonitrate group concentrations in submicron particles with high nitrate and organic fractions in coastal southern California. Atmospheric Environment 44, 1970–1979.

Doney, S.C., Mahowald, N., Lima, I., Feely, R.A., Mackenzie, F.T., Lamarque, J-F., and Rasch, P.J., 2007. Impact of anthropogenic atmospheric nitrogen and sulfur deposition on ocean acidification and the inorganic carbon system. Proceedings of the national academy of Science 104, 14580-14585.

Elbert, W., Taylor, P.E., Andreae, M.O., Poschl, U., 2007. Contribution of fungi to primary biogenic aerosols in the atmosphere:wet and dry discharded spores, carbohydrates, and inorganic ions. Atmospheric Chemistry and Physics 7, 4569-4588.

Epstein, S.A., Blair, S.L., Nizkorodov, S.A., 2014. Direct photolysis of α-pinene ozonolysis secondary organic aerosol: effect on particle mass and peroxide content. Environmental Science and Technology 48, 11251-11258.

Fehsenfeld, F.C., Dickerson, R.R., Hubler, G., Luke, W.T., Nunnermacker, L.J., Williams, E.J., Roberts, J.M., Calvert, J.G., Curran, C.M., Delany, A.C., Eubank, C.S., Fahey, D.W., Fried, A., Grandrud, B.W., Langford, A.O., Murphy, P.C., Norton, R.B., Pickering, K.E., Ridley, B.A., 1987. A ground-based intercomparison of NO, NOx and NOy measurement techniques. Journal of Geophysical Research 92, 14710-14722.

Gaston, C.J., Lopez-Hifiker, F.D., Whybrew, L.E., Hadley, O., McNair, F., Gao, H., Jaffe, D.A., Thornton, J.A., 2016. Online molecular characterization of fine particulate matter in Port Angels, WA: Evidence for a major impact from residential wood smoke. Atmospheric Environment 138, 99-107.

Gomez-Gonzalez, Y., Surratt, J. D., Cuyckens, F., Szmigielski, R.,Vermeylen, R., Jaoui, M., Lewandowski, M., Offenberg, J. H., Kleindienst, T. E., Edney, E. O., Blockhuys, F., Van Alsenoy, C.,Maenhaut, W., and Claeys, M.,2008. Characterization of organosulfates from the photooxidation of isoprene and unsaturated fatty acids in ambient aerosol using liquid chromatography/(-) electrospray ionization mass spectrometry, Journal of Mass Spectrometry, 43, 371–382.

Gomez-Gonzalez, Y., Wang, W., Vermeylen, R., Chi, X., Neirynck, J., Janssens, I.A., Maenhaut, W., Claeys, M., 2012. Chemical characterization of atmospheric aerosols during a 2007 summer field campaign at Brasschaat, Belgium: sources and source processes of biogenic secondary organic aerosol. Atmospheric Chemistry and Physics 12, 125-138.

Gonzalez Benitez, J.M., Cape, J.N., Heal, M.R., van Dijk, N., Vidal Diez, A., 2009. Atmospheric nitrogen deposition in south-east Scotland: Quantification of the organic nitrogen fraction in wet, dry and bulk deposition. Atmospheric Environment 43, 4087-4094.

Hamilton, J.F., Alfarra, M.R., Robinson, N., Ward, M.W., Lewis, A.C., McFiggans, G.B., Coe, H., Allan, D., 2013. Linking biogenic hydrocarbons to biogenic aerosol in the Borneo rainforest. Atmospheric Chemistry and Physics 13, 11295-11305.

He, Q-F., Ding, X., Wang, X-M., Yu, J.Z., Fu, X-X., Liu, T-Y., Zhang, Z., Xue, J., Chen, D-H., Zhong, L-J., Donadue, N.M., 2014. Organosulfates from pinene and isoprene over the Pearl River Delata, South China: Seasonal variation and implication in formation mechanisms. Environmental Science and Technology 48, 9236-9245.

Hecobian, A., Zhang, X., Zheng, M., Frank, N., Edgerton, E.S., Weber, R.J., 2010. Water Soluble Organic Aerosol material and the light-absorption characteristics of aqueous extracts measured over the Southeastern United States. Atmospheric Chemistry and Physics **10**, 5965-5977.

Hemann, J.G., Brinkman, G.L., Dutton, S.J., Hannigan, M.P., Milford, J.B., Miller, S.L., 2009. Assessing positive matrix factorization model fit: a new method to estimate uncertainty and bias in factor contributions at the measurement time scale. Atmospheric Chemistry and Physics 9, 497-513.

Hungate, B.A., Dukes, J.S., Shaw, M.R., Luo, Y., and Field C.B., 2003. Nitrogen and Climate Change. Science 302, 1512-1513.

Iinuma, Y., Boge, O., Kahnt, A., Herrmann,H., 2009. Laboratory chamber studies on the formation of organosulfates from reactive uptake of monoterpene oxides. Physical Chemistry Chemical Physics 11, 7985-7997.

Iinuma, Y., Boge, O., Grafe, R., Herrmann, H., 2010. Methyl-nitrocatechols : atmospheric tracers compounds for biomass burning secondary organic aerosols. Environmental Science and Technology 44, 8453-8459.

Iinuma, Y., Keywood, M., Herrmann, H., 2016. Characterization of primary and secondary organic aerosols in Melbourne airshed: The influence of biogenic emissions, wood smoke and bushfires. Atmospheric Environment 130, 54-63.

Jickells, T., Baker, A.R., Cape, J.N., Cornell, S.E., Nemitz, E., 2013. The cycling of organic nitrogen through the atmosphere. Philosophical Transactions of the Royal Society B 368:20130115.

Kahnt, A., Behrouzi, S., Vermeylen, R., Safi Shalamzari, M., Vercauteren, J., Roekens, E., Claeys, M., Maenhaut, W., 2013. One-year study of nitro-organic compounds and their relation to wood burning in PM10 aerosol from a rural site in Belgium. Atmospheric Environment 81, 561-568.

Kahnt, A., Iinuma, Y., Blockhuys, F., Mutzel, A., Vermeylen, R., Kleindienst, T.E., Jaoui, M., Offenberg, J.H., Lewandowski, M., Boge, O., Herrmann, H., Maenhaut, W., Claeys, M., 2014. 2-Hydroxyterpenylic acid: an oxygenated marker compound for α-pinene secondary organic aerosolin ambient fine aerosol. Environmental Science and Technology 48, 4901-4908.

Kanakidou, M., Duce, R.A., Prospero, J.M., Baker, A.R., Benitez-Nelson, C., Dentener, F.J., Hunter, K.A., Liss, P.S., Mahowald, N., Okin, G.S., Sarin, M., Tsigaridis, K., Uematsu, M., Zamora, L.M., Zhu, T., 2012. Atmospheric fluxes of organic N and P to the global ocean. Global Biogeochemical Cycles 26, GB3026, doi:10.1029/2011GB004277.

Keene, W.C., Montag, J.A., Maben, J.R., Southwell, M., Leonard, J., Church, T.M., Moody, J.L., Galloway, J.N., 2002. Organic nitrogen in precipitation over Eastern North America. Atmospheric Environment 36, 4529-4540.

Kitanovski, Z., Grgic, I., Vermeylen, R., Claeys, M., Maenhaut, W., 2012. Liquid chromatography tandem mass spectrometry method for characterization of monoaromatic nitro-compounds in atmospheric particulate matter. Journal of Chromatography A 1268, 35-43.

Kleindienst, T. E., Jaoui, M., Lewandowski, M., Offenberg, J.H., Lewis, C.W., Bhave, P.V., Edney, E.O., 2007. Estimates of the contributions of biogenic and anthropogenic hydrocarbons to secondary organic aerosol at a southeastern US location. Atmospheric Environment 41, 8288-8300.

Lee, B.H., Mohr, C., Lopez-Hilfiker, F.D., Lutz, A., Hallquist, M., Lee, L., Romer, P., Cohen, R.C., Lyer, S., Kurten, T., Hu,W., Day,D.A., Campuzano-Jost, P., Jimenez, J.L., Xu, L., Ng, N.L., Guo,H., Weber,R.J., Wild, R.J., Brown,S.S., Koss, A., de Gouw, J., Olson, K., Goldstein, A.H., Seco, R., Kim, S., McAvery, K., Shepson, P.B., Starn, T., Baumann, K., Edgerton, E.S., Liu, J., Shilling, J.E., Miller, D.O., Brune, W., Schobesberger,S., DAmbro, E.L., Thornton, J.A., 2016. Highly functionalized organic nitrates in the southeast United States: Contribution to secondary organic aerosol and reactive nitrogen budgets. Proceedings of the National Academy of Science 113, 1516-1521.

Lin, M., Walker, J., Geron, C., Khlystov, A., 2010. Organic nitrogen in PM2.5 aerosol at a forest site in the Southeast US. Atmospheric Chemistry and Physics 10, 2145-2157.

Lin, Y-H., Zhang, H., Pye, H.O.T., Zhang, Z., Marth, W.J., Park, S., Arashiro, M., Cui, T., Hapsari Budisulistiorini, S., Sexton, K.G., Vizuete, W., Xie, Y., Luecken, D.J., Piletic, I.R., Edney, E.O., Bartolotti, L.J., Gold, A., Surratt, J.D., 2013a. Epoxide as a precursor to secondary organic aerosol formation from isoprene photooxidation in the presence of nitrogen oxides. Proceedings of the National Academy of Science 110, 6718-6723.

Lin, Y-H., Knipping, E.M., Edgerton, E.S., Shaw, S.L., Surratt, J.D., 2013b. Investigating the influences of SO_2 and NH_3 levels on isoprene-derived secondary organic aerosol formation using conditional sampling approaches. Atmospheric Chemistry and Physics 13, 8457-8470.

Liu, J., Bergin, M., Guo, H., King, L., Kotra, N., Edgerton, E., Weber, R.J., 2013. Size-resolved measurements of brown carbon in water and methanol extracts and estimates of their contribution to ambient fine-particle light absorption. Atmospheric Chemistry and Physics 13, 12389-12404.

Liu, J., Scheuer, E., Dibb, J., Diskin, G.S., Ziemba, L.D., Thornhill, K.l., Anderson, B.E., Wisthaler, A., Mikoviny, T., Devi, J.J., Bergin, M., Perring, A.E., Markovic, M.Z., Scheartz, J.P., Campuzano-Jost, P., Day, D.A., Jimenez, J.L., Weber, R.J., 2015. Brown carbon aerosol in the North American continental troposphere: sources, abundance, and radiative forcing. Atmospheric Chemistry and Physics 15, 7841-7858.

Lohse, K.A., Hope, D., Sponseller, R., Allen, J.O., Grimm, N.B., 2008. Atmospheric deposition of carbon and nutrients across an arid metropolitan area. Science of the Total Environment 402, 95-105.

Magnani, F., Mencuccini, M., Borghetti, M., Berbigier, P., Berninger, F., Delzon, S., Grelle, A., Hari, P., Jarvis, P.G., Kolari, P., Kowalski, A.S., Lankreijer, H., Law, B.E., Lindroth, A., Loustau, D., Manca, G., Moncrieff, J.B., Rayment, M., Tedeschi, V., Valentini, R., Grace, J., 2007. The human footprint in the carbon cycle of temperate and boreal forests. Nature 447, 848-850.

Meade, L.E., Riva, M., Blomberg, M.Z., Brock, A.K., Qualters, E.M., Siejack, R.A., Ramakrishnan, K., Surratt, J.D., Kautzman, K.E., 2016. Seasonal variation of fine particulate organiosulfates derived from biogenic and anthropogenic hydrocarbons in the mid-Atlantic

United States. Atmospheric Environment 145, 405-414.

Miniat, C.F., Laseter, S.H., Swank, W.T., Swift, L.W. Jr., 2015. Daily air temperature, relative humidity, vapor pressure, PPFD, wind speed and direction for climate stations at the Coweeta Hydrologic Lab, North Carolina. Fort Collins, CO: Forest Service Research Data Archive. Updated 28 February 2017. https://doi.org/10.2737/RDS-2015-0042

Miyazaki, Y., Fu, P., Ono, K., Tachibana, E., Kawamura, K., 2014. Seasonal cycles of water-soluble organic nitrogen aerosols in a deciduous broadleaf forest in northern Japan. Journal of Geophysical Research: Atmospheres 119, 1440-1454.

Mohr, C., Lopez-Hilfiker, F.D., Zotter, P., Prevot, A.S.H., Xu, L., Ng, N.L., Herndon, S.C., Williams, L.R., Franklin, J.P., Zahniser, M.S., Worsnop, D.R., Knighton, W.B., Aiken, A.C., Gorkowski, K.J., Dubey, M.K., Allan, J.D., Thornton, J.A., 2013. Contribution of nitrated phenols to wood burning brown carbon light absorption in Detling, United Kingdom during winter time. Environmental Science and Technology 47, 6316-6324.

Muller, L.; Reinnig, M.-C.; Naumann, K. H.; Saathoff, H.; Mentel, T. F.; Donahue, N. M.; Hoffmann, T.,2012. Formation of 3-methyl-1,2,3- butanetricarboxylic acid via gas phase oxidation of pinonic acid – a mass spectrometric study of SOA aging. Atmospheric Chemistry and Physics 12, 1483−1496.

Neff, J.C., Holland, E.A., Dentener, F.J., Mcdowell, W.H., Russell, K.M., 2002a. The origin, composition and rates of organic nitrogen depiction: A missing piece of the nitrogen cycle? Biogeochemistry 57/58, 99-136.

Neff, J.C., Townsend, A.R., Gleixner, G., Lehman, S.J., Turnbull, J., Bowman, W., 2002b. Variable effects of nitrogen additions on the stability and turnover of soil carbon. Nature 419, 915-917.

Oishi, A.C., Miniat, C.F., Novick, K.A., Brantley, S.T., Vose, J.M., Walker, J.T., 2017. Warmer temperatures reduce net carbon uptake, but do not affect water use, in a mature southern Appalachian forest. Agricultural and Forest Meteorology. In press.

Ollinger, S.V., Aber, J.D., Reich, P.B., Freuder, R.J., 2002. Interactive effects of nitrogen deposition, tropospheric ozone, elevated CO2 and land use history on the carbon dynamics of northern hardwood forests. Global Change Biology 8, 545-562.

Paatero, P. User's Guide for Positive Matrix Factorization Program PMF2 and PMF3, Part 1: Tutorial. University of Helsinki: Helsinki, Finland, 1998a.

Paatero, P. User's Guide for Positive Matrix Factorization Program PMF2 and PMF3, Part 2: Reference. University of Helsinki: Helsinki, Finland, 1998b.

Place, B. K., Quilty, A. T., Di Lorenzo, R. A., Ziegler, S. E., and VandenBoer, T. C. ,2017. Quantitation of 11 alkylamines in atmospheric samples: separating structural isomers by ion

chromatography, Atmospheric Measurement Techniques 10, 1061–1078.

Pregitzer, K.S., Burton, A.J., Zak, D.R., and Talhelm, A.F., 2008. Simulated chronic nitrogen deposition increases carbon storage in Northern Temperate forests. Global Change Biology 14, 142-153.

Romer, P. S., Duffey, K. C., Wooldridge, P. J., Allen, H. M., Ayres, B. R., Brown, S. S., Brune, W. H., Crounse, J. D., de Gouw, J., Draper, D. C., Feiner, P. A., Fry, J. L., Goldstein, A. H., Koss, A., Misztal, P. K., Nguyen, T. B., Olson, K., Teng, A. P., Wennberg, P. O., Wild, R. J., Zhang, L., and Cohen, R. C.,2016. The lifetime of nitrogen oxides in an isoprene-dominated forest, Atmospheric Chemistry and Physics 16, 7623-7637.

Samy, S., Robinson, J., Rumsey, I.C., Walker, J.T., Hays, M.D.,2013. Speciation and trends of organic nitrogen in southeastern U.S. fine particulate matter ($PM_{2.5}$). Journal of Geophysical Research: Atmospheres 118, 1996-2006.

Shalamzari, M.S., Vermeylen, R., Blockhuys, F., Kleindienst, T.E., Lewandowski, M., Szmigielski, R., Rudzinski, K.J., Spolnik, G., Danikiewicz, W., Maenhaut, W., Claeys, M., 2016. Characterization of polar organosulfates in secondary organic aerosol from the unsaturated aldehydes 2-E-pentenal, 2-E-hexenal, and 3-Z-hexenal. Atmospheric Chemistry and Physics 16, 7135-7148.

Simkin, S.M., Allen, E.B., Bowman, W.D., Clark, C.M., Belnap, J., Brooks, M.L., Cade, B.S., Collins, S.L., Geiser, L.H., Gilliam, F.S., Jovan, S.E., Pardo, L.H., Schulz, B.K., Stevens, C.J., Suding, K.N., Throop, H.L., and Waller, D.M., 2016. Conditional vulnerability of plant diversity to atmospheric nitrogen deposition across the United States. Proceedings of the national academy of Science 113, 4086-4091.

Surratt, J. D., Murphy, S.M., Kroll, J.H., Ng, N.L., Hildebrandt, L., Sorooshian, A., Szmigielski, R., Vermeylen, R., Maenhaut, W., Claeys, M., Flagen, R.C., Seinfeld, J.H., 2006. Chemical composition of secondary organic aerosol formed from the photooxidation of isoprene. Journal of Physical Chemistry A 110, 9665-9690.

Surratt, J.D., Kroll, J.H., Kleindienst, T.E., Edney, E.O., Claeys, M., Sorooshian, A., Ng, N.L., Offenberg, J.H., Lewandowski, M., Jaoui, M., Flagan, R.C., Seinfeld, J.H., 2007. Evidence for organosulfates in secondary organic aerosol. Environmental Science and Technology 41, 517-527.

Surratt, J.D., Gomez-Gonzalez, Y., Chan, A.W.H., Vermeylen, R., Shahgholi, M., Kleindienst, T.E., Edney, E.O., Offernberg, J.H., Lewandowski, M., Jaoui, M., Maenhaut, W., Claeys, M., Flagan, R.C., Seinfeld, J.H., 2008. Organosulfate formation in biogenic organic aerosol. Journal of physical chemistry A 112, 8345-8378.

Surratt, J.D., Chan, A.W.H., Eddingsaas, N.C., Chan, M.N., Loza, C.L., Kwan, A.J., Hersey, S.P., Flagan, R.C., Wennberg, P.O., Seinfeld, J.H., 2010. Reactive intermediates revealed in secondary organic aerosol formation from isoprene. Proceedings of the National Academy of

977 Science 107, 6640-6645.
978
979 Swank, W.T. and D.A. Crossley, Jr..1988. Introduction and site description. In Forest Hydrology
980 and Ecology at Coweeta. 169 pp. Edited by W.T. Swank and D.A. Crossley, Jr. Springer-Verlag,
981 Berlin.
982
983 Swift, L.W..Jr., G.B. Cunningham and J.E. Douglass. 1988. Climatology and Hydrology. In
984 Forest Hydrology and Ecology at Coweeta. 469 pp. Edited by W.T. Swank and D.A. Crossley.
985 Jr. Springer-Verlag. Berlin
986
987 Szmigielski, R.; Surratt, J. D.; Gómez-González, Y.; Van der Veken, P.; Kourtchev, I.;
988 Vermeylen, R.; Blockhuys, F.; Jaoui, M.; Kleindienst, T. E.; Lewandowski, M.; Offenberg, J. H.;
989 Edney, E. O.; Seinfeld, J. H.; Maenhaut, W.; Claeys, M., 2007. 3-methyl-1,2,3-
990 butanetricarboxylic acid: An atmospheric tracer for terpene secondary organic aerosol.
991 Geophysical Research Letter 34, L24811.
992
993 U.S. EPA, 2017. U.S. Environmental Protection Agency Clean Air Markets Division,
994 Clean Air Status and Trends Network (CASTNET). Hourly ozone and meteorology.
995 Available at www.epa.gov/castnet. Date accessed: 01/15/2017.
996
997 Walker, J.T., Dombek, T.L., Green,L.A., Gartman,N., Lehmann, C.M.B., 2012. Stability of
998 organic nitrogen in NADP wet deposition samples. Atmospheric Environment 60, 573-582.
999
1000 Williams, E.J.; Baumann, K.; Roberts, J.M.; Bertman, S.B.; Norton, R.B.; Fehsenfeld, F.C.;
1001 Springston, S.R.; Nunnermacker, L.G.; Newman, L.; Olszyna, K; Meagher, J.; Hartsell, B.;
1002 Edgerton, E.; Perason, J.R.; Rodgers, M.O., 1998. Intercomparison of ground-based NOy
1003 measurements techniques. Journal of Geophysical Research: Atmospheres 103, 22261-22280.
1004
1005 Worton, D. R., Goldstein, A. H., Farmer, D. K., Docherty, K. S., Jimenez, J. L., Gilman, J. B.,
1006 Kuster, W. C., de Gouw, J., Williams, B. J., Kreisberg, N. M., Hering, S. V., Bench, G., McKay,
1007 M., Kristensen, K., Glasius, M., Surratt, J. D., Seinfeld, J. H., 2011. Origins and composition of
1008 fine atmospheric carbonaceous aerosol in the Sierra Nevada Mountains, California. Atmospheric
1009 Chemistry and Physics 11, 10219−10241.
1010
1011 Worton, D.R., Surratt, J.D., LaFranchi, B.W., Chan, A.W.H., Zhao, Y., Weber, R.J., Park, J-H.,
1012 Gilman, J.B., de Gouw, J., Park, C., Schade, G., Beaver, M., St. Clair, J.M., Crounse, J.,
1013 Wennberg, P., Wolfe, G.M., Harrold, S., Thornton, J.A., Farmer, D.K., Docherty, K.S., Cubison,
1014 M.J.M., Jimenez, J-L., Frossard, A.A., Russell, L.M., Kristensen, K., Glasius, M., Mao, J., Ren,
1015 X., Brune, W., Browne, E.C., Pusede, S.E., Cohen, R.C., Seinfeld, J.H., Goldstein, A.H., 2013.
1016 Observational insights into aerosol formation from isoprene. Environmental Science and
1017 Technology 47, 11403-11413.
1018
1019 Xie, M., Hannigan, M.P., Dutton, S.J., Milford, J.B., Hemann, J.G., Miller, S.L., Schauer, J.J.,
1020 Peel, J.L., Vedal, S., 2012. Positive matrix factorization of PM2.5: Comparison and implications
1021 of using different speciation data sets. Environmental Science & Technology 46, 11962-11970
1022

1023 Xie, M., Barsanti, K.C., Hannigan, M.P., Dutton, S.J., Vedal, S., 2013. Positive matrix
1024 factorization of PM2.5 - eliminating the effects of gas/particle partitioning of semivolatile
1025 organic compounds. Atmospheric Chemistry and Physics 13, 7381-7393.
1026
1027 Xie, M., Hannigan, M.P., Barsanti, K.C., 2014. Impact of Gas/Particle Partitioning of
1028 Semivolatile Organic Compounds on Source Apportionment with Positive Matrix Factorization.
1029 Environmental Science & Technology 48, 9053-9060.
1030
1031 Zellweger, C., Ammann, M., Buchmann, B., Hofer, P., Lugauer, M., Ruttimann, R., Streit, N.,
1032 Weingartner, E., Baltensperger, U., 2000. Summertime NOy speciation at the Jungfraujoch,
1033 3580m above sea level, Switzerland. Journal of Geophysical Research 105, 6655-6667.
1034
1035 Zhang, Y., Song, L., Liu, X.J., Li, W.Q., Lu, S.H., Zheng, L.X., Bai, Z.C., Cai, G.Y., Zhang,
1036 F.S., 2012. Atmospheric organic nitrogen deposition in China. Atmospheric Environment 46,
1037 195-204.

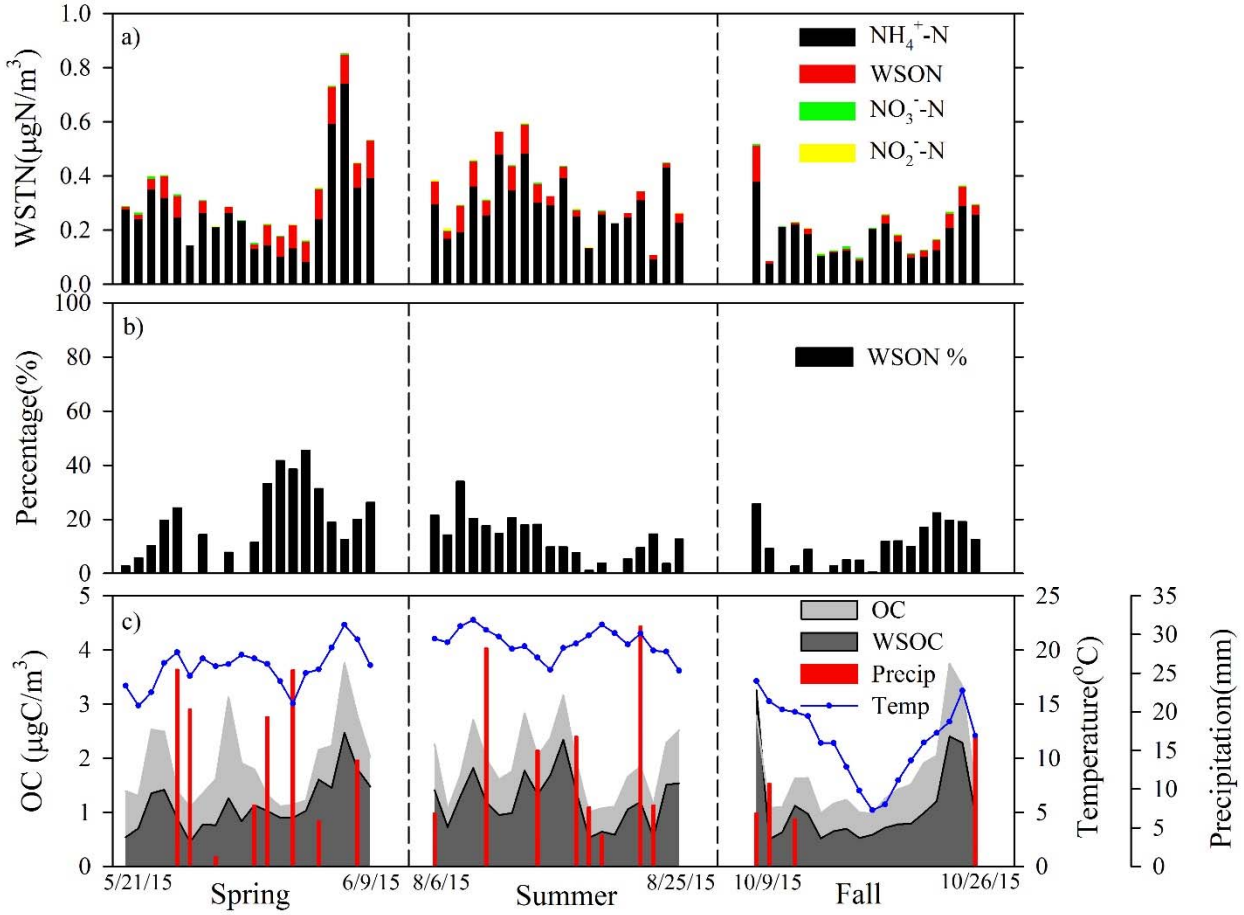

Figure 1. a) Individual concentrations of nitrogen components to WSTN (NH_4^+, NO_3^-, NO_2^- and WSON); b) Percent contribution of WSON to WSTN; c) Time series of OC, WSOC, temperature and precipitation. Start and end dates of each intensive sampling periods are shown.

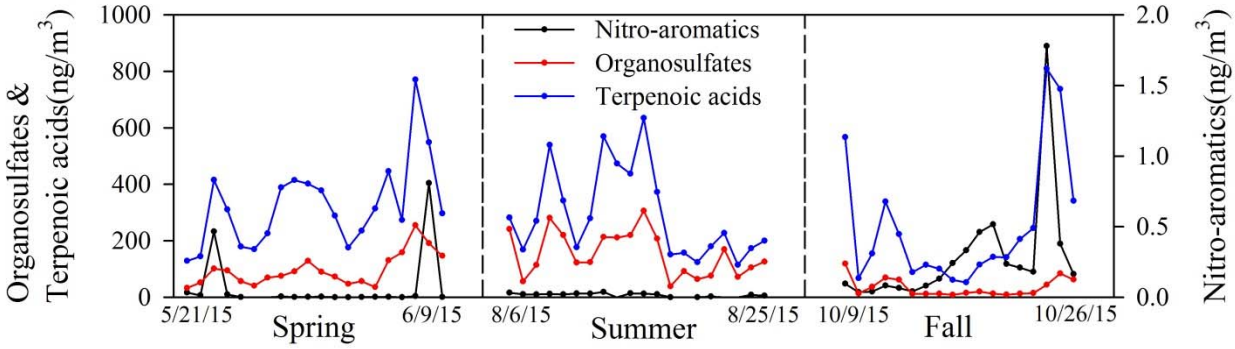

Figure 2. Time series of summed compound group concentrations of nitro-aromatics, organosulfates and terpenoic acids.

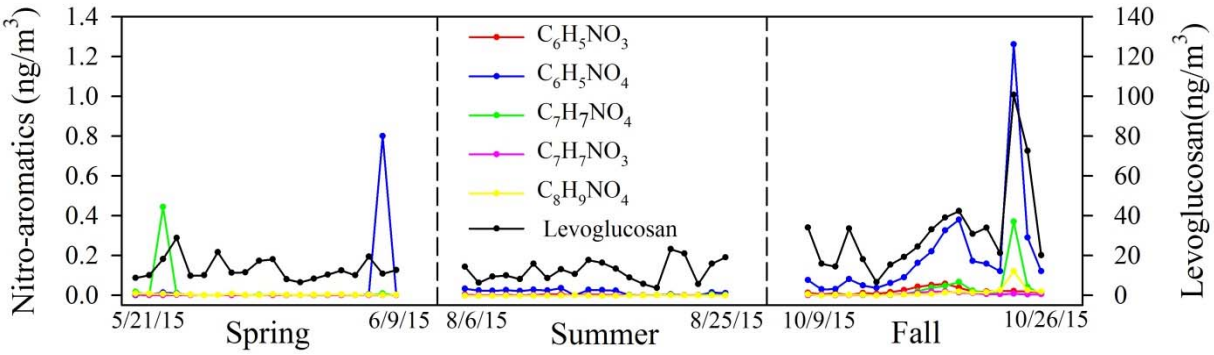

Figure 3. Time series of individual nitro-aromatics compounds as well as levoglucosan.

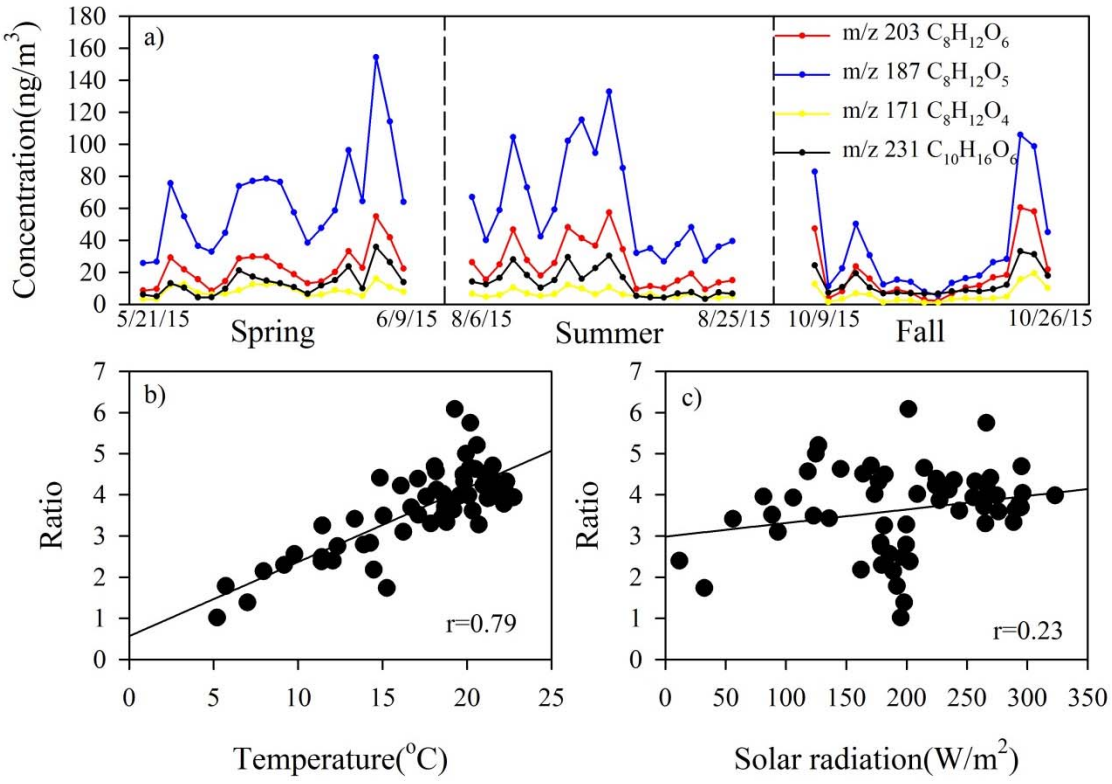

Figure 4. a) Time series of these four identified terpenoic acids(3-methyl-1,2,3-butanetricarboxylic acid(MBTCA, $C_8H_{12}O_6$, m/z 203), 2-hydroxyterpenylic acid($C_8H_{12}O_5$, m/z 187), terpenylic acid($C_8H_{12}O_4$, m/z 171) and Diaterpenylic acid acetate(DTAA, $C_{10}H_{16}O_6$,m/z 231)); b) correlation of concentration ratios of higher generation oxidation products($C_8H_{12}O_6$, m/z 203 and $C_8H_{12}O_5$, m/z 187) to early oxidation fresh SOA products($C_8H_{12}O_4$, m/z 171 and $C_{10}H_{16}O_6$,m/z 231) with temperature and ; c) with solar radiation.

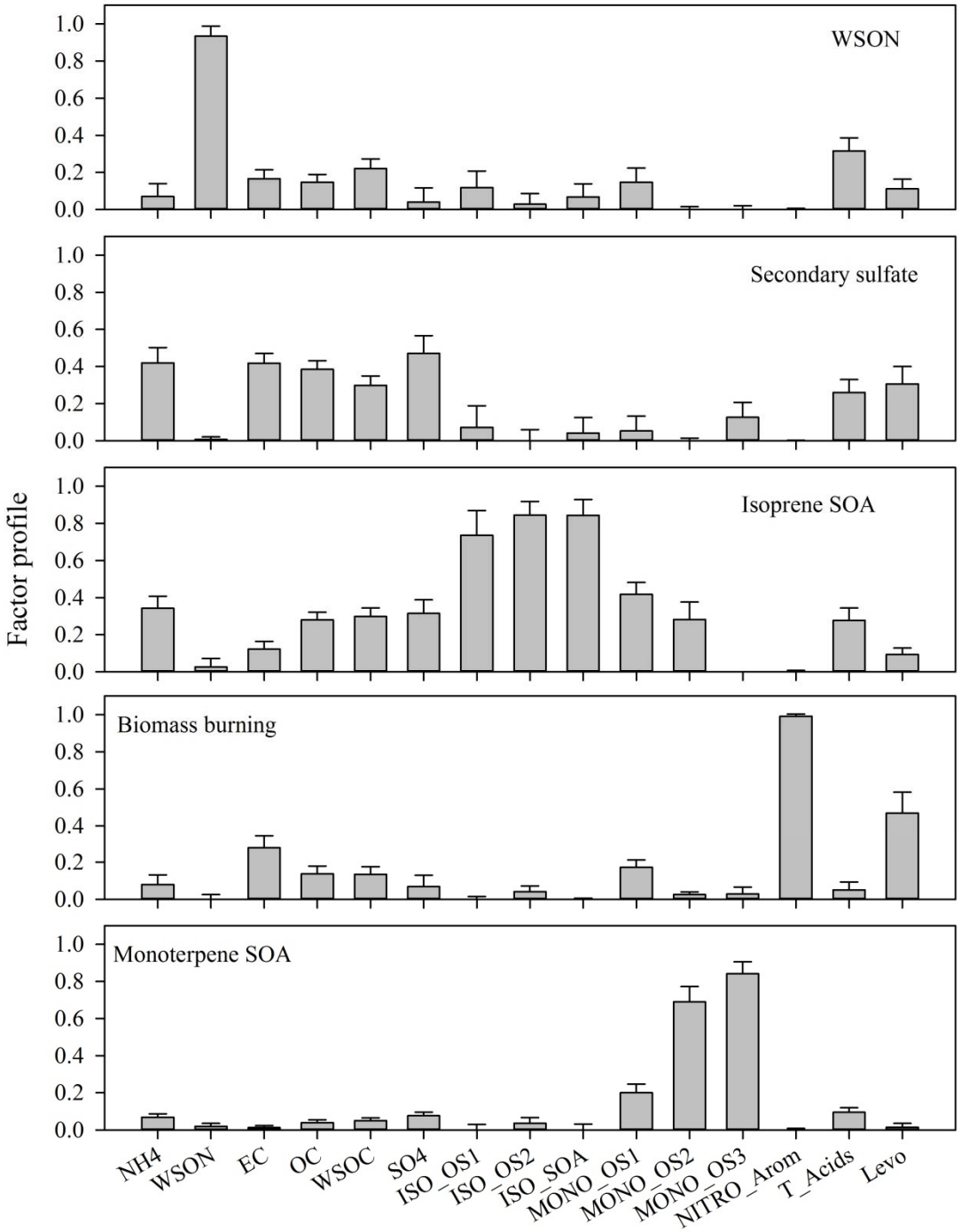

Figure 5. Normalized factor profiles (error bar represents one standard deviation).

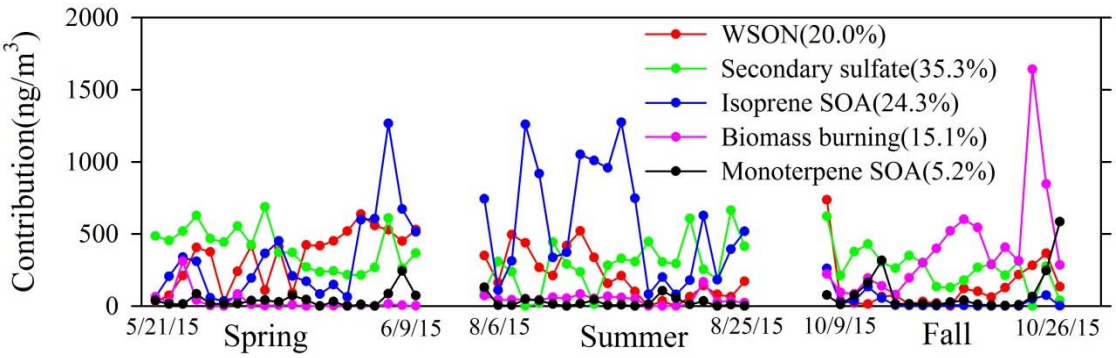

Figure 6. Time series of factor contributions to WSOC (mean factor contribution shown in brackets).

Table 1. Summary of particulate and gaseous species measured at Coweeta sampling site in 2015.

	Spring				Summer				Fall			
($\mu g/m^3$)	mean	median	min	max	mean	median	min	max	mean	median	min	max
OM (OC*2)	3.77	3.41	2.18	7.52	3.80	3.79	2.00	6.32	3.36	2.85	1.96	7.49
EC	0.05	0.05	0.03	0.10	0.05	0.05	0.02	0.08	0.07	0.07	0.03	3.75
WSOC	1.14	1.03	0.45	2.47	1.22	1.24	0.53	2.34	1.09	0.78	0.50	3.25
WSTN	0.33	0.29	0.14	0.86	0.34	0.32	0.11	0.59	0.21	0.20	0.08	0.52
WSON	0.06	0.07	ND	0.14	0.05	0.03	ND	0.11	0.03	0.02	ND	0.13
NH_4^+ -N	0.27	0.24	0.08	0.74	0.29	0.28	0.09	0.48	0.18	0.17	0.08	0.38
NO_3^- -N	0.00	0.00	ND	0.01	0.00	0.00	ND	0.01	0.00	0.00	ND	0.01
NO_2^- -N	0.00	0.00	ND	0.00	0.00	0.00	ND	0.01	0.00	0.00	ND	0.00
SO_4^{2-}	0.99	0.93	0.26	2.44	1.01	0.95	0.31	1.85	0.63	0.58	0.30	1.33
O_3(ppb)	25.1	21.6	13.9	46.1	15.8	15.8	9.0	22.8	19.4	20.5	11.1	26.9
NOx(ppb)	0.75	0.79	0.45	1.03	0.54	0.58	0.24	0.91	0.65	0.68	0.43	0.89
Temp(^{o}C)	18.4	18.6	14.8	22.3	20.7	20.6	18.1	22.8	11.6	11.7	5.2	17.1
RH%	81.7	84.9	61.0	94.8	82.1	83.1	71.9	88.5	77.7	74.9	65.1	92.0
Radiation	235	265	81	296	205	201	106	323	151	180	12	203

Table 2. Spearman rank correlation coefficients among measured species and meteorological variables by season. Nitro-aromatics (Nitro), Organosulfates (OS), and terpenoic acids (Tacids) represent group summed concentrations.

Spring	OC	WSOC	NO_3^-	NH_4	SO_4^{2-}	WSON	Abs_{365}	Nitro	OS	Tacids	O_3	NOx	Temp	RH	radiation	Precip
EC	**0.853**	0.474	0.177	**0.690**	**0.705**	0.129	**0.875**	**0.583**	**0.645**	**0.579**	0.430	0.263	0.364	**-0.627**	0.520	-0.458
OC		**0.737**	0.069	**0.767**	**0.708**	0.328	**0.773**	0.541	**0.848**	**0.761**	0.275	0.498	0.543	-0.408	0.441	-0.315
WSOC			0.105	0.523	0.429	**0.768**	0.424	0.241	**0.805**	**0.723**	0.185	0.543	0.472	-0.059	0.135	-0.145
NO_3^-				0.15	0.137	0.129	0.108	0.492	-0.104	-0.051	0.559	0.084	-0.203	**-0.564**	0.362	-0.169
NH_4					**0.944**	0.457	**0.842**	0.355	**0.684**	0.298	0.474	0.189	0.439	-0.510	0.441	-0.362
SO_4^{2-}						0.400	**0.827**	0.277	**0.642**	0.229	0.457	0.051	0.540	-0.526	0.374	-0.306
WSON							0.215	-0.113	0.522	0.236	0.215	0.140	0.326	0.080	-0.105	0.055
Abs_{365}								0.456	**0.591**	0.349	0.495	0.174	0.254	**-0.612**	0.507	-0.529
Nitro[1]									0.278	0.426	0.493	0.319	0.021	-0.537	0.307	-0.177
OS[2]										**0.759**	0.080	0.341	**0.644**	-0.084	0.162	-0.140
Tacids[3]											-0.066	**0.571**	0.442	0.000	0.141	-0.066
O_3												0.068	0.026	**-0.797**	0.453	-0.219
NOx													0.227	-0.068	0.257	-0.165
Temp														-0.111	0.183	0.061
RH															**-0.786**	0.551
Radiation																**-0.734**

[1]nitro-aromatics; [2]organosulfates; [3]terpenoic acids; values in bold indicate $p<0.01$

Summer	OC	WSOC	NO_3^-	NH_4	SO_4^{2-}	WSON	Abs_{365}	Nitro	OS	Tacids	O_3	NOx	Temp	RH	radiation	Precip
EC	**0.671**	**0.659**	0.113	**0.626**	0.555	**0.562**	0.546	**0.576**	0.474	0.537	0.325	0.242	-0.402	-0.384	0.465	-0.356
OC		**0.961**	0.233	**0.627**	0.517	0.556	0.558	0.523	**0.856**	**0.823**	0.304	0.289	-0.379	-0.300	0.269	-0.189
WSOC			0.263	**0.592**	0.490	0.549	0.397	**0.564**	**0.820**	**0.835**	0.247	0.238	-0.302	-0.325	0.259	-0.269
NO_3^-				0.343	0.271	0.355	-0.143	0.165	0.325	0.469	**0.642**	**0.665**	0.120	-0.279	0.263	0.181
NH_4					**0.977**	0.550	0.405	0.535	**0.609**	**0.585**	0.320	0.415	-0.108	-0.388	0.421	-0.218
SO_4^{2-}						0.465	0.343	0.477	0.487	0.474	0.241	0.350	-0.090	-0.426	0.447	-0.290
WSON							0.170	**0.633**	**0.642**	**0.692**	**0.698**	0.391	0.026	**-0.637**	0.555	-0.201
Abs_{365}								0.086	0.423	0.278	0.149	0.140	**-0.586**	0.012	0.167	0.089
Nitro									**0.573**	**0.614**	0.367	0.418	-0.116	-0.346	0.247	-0.446
OS										**0.905**	0.338	0.472	-0.080	-0.175	0.098	0.087
Tacids											0.432	0.531	-0.150	-0.263	0.138	-0.035
O_3												**0.621**	-0.045	**-0.607**	**0.571**	-0.046
NOx													-0.116	-0.049	0.018	0.214
Temp														-0.097	-0.012	0.172
RH															**-0.919**	**0.607**
Radiation																**-0.583**

Table 2. Continued.

Fall	OC	WSOC	NO_3^-	NH_4	SO_4^{2-}	WSON	Abs_{365}	Nitro	OS	Tacids	O_3	NOx	Temp	RH	radiation	Precip
EC	**0.719**	**0.695**	0.449	0.216	0.127	**0.707**	**0.897**	**0.779**	0.154	0.472	0.042	0.106	-0.036	-0.044	-0.100	-0.380
OC		**0.955**	0.077	0.434	0.333	**0.837**	**0.715**	0.340	0.554	**0.897**	-0.282	-0.189	0.525	0.441	-0.441	0.047
WSOC			0.092	**0.593**	0.494	**0.816**	**0.668**	**0.362**	**0.649**	**0.922**	-0.222	-0.152	0.474	0.422	-0.470	0.146
NO_3^-				-0.044	-0.053	0.106	0.385	0.445	-0.300	-0.088	0.257	0.084	-0.375	-0.461	0.265	-0.385
NH_4					**0.983**	0.490	0.191	0.209	**0.874**	**0.664**	-0.158	-0.096	0.356	0.350	-0.410	0.265
SO_4^{2-}						0.399	0.100	0.152	**0.833**	0.571	-0.110	-0.086	0.313	0.290	-0.342	0.244
WSON							**0.789**	0.486	0.546	**0.746**	-0.143	0.036	0.364	0.441	-0.538	0.224
Abs_{365}								**0.802**	0.110	0.494	0.150	0.286	-0.096	0.011	-0.226	-0.273
Nitro									0.001	0.187	0.313	0.445	-0.455	-0.226	0.009	-0.378
OS										**0.746**	-0.350	-0.356	**0.659**	0.573	-0.581	0.466
Tacids											-0.401	-0.249	**0.653**	**0.628**	-0.587	0.241
O_3												**0.664**	**-0.746**	**-0.820**	**0.602**	-0.340
NOx													**-0.719**	-0.418	0.389	-0.303
Temp														**0.787**	**-0.639**	0.490
RH															**-0.847**	**0.638**
Radiation																**-0.640**

Overall	OC	WSOC	NO_3^-	NH_4	SO_4^{2-}	WSON	Abs_{365}	Nitro	OS	Tacids	O_3	NOx	Temp	RH	radiation	Precip
EC	**0.545**	**0.422**	**0.361**	0.214	0.216	0.175	**0.753**	**0.642**	-0.041	0.283	0.338	0.308	**-0.396**	**-0.500**	0.131	**-0.449**
OC		**0.928**	0.087	**0.672**	**0.611**	**0.585**	**0.615**	0.181	**0.698**	**0.828**	0.016	0.167	0.281	-0.017	0.207	-0.115
WSOC			0.110	**0.643**	**0.564**	**0.726**	**0.444**	0.120	**0.729**	**0.848**	-0.025	0.116	0.325	0.102	0.172	-0.054
NO_3^-				0.002	0.018	0.161	0.200	0.310	-0.190	0.097	**0.536**	**0.384**	-0.322	**-0.433**	0.189	-0.127
NH_4					**0.976**	**0.543**	**0.358**	-0.063	**0.794**	**0.567**	0.071	0.053	**0.528**	-0.061	0.313	-0.061
SO_4^{2-}						**0.493**	0.348	-0.103	**0.733**	**0.502**	0.107	0.029	**0.517**	-0.107	**0.339**	-0.072
WSON							0.272	-0.061	**0.575**	**0.590**	0.233	0.185	**0.356**	0.103	0.283	0.044
Abs_{365}								**0.372**	0.127	0.294	0.303	0.260	-0.218	-0.290	0.100	-0.255
Nitro									-0.302	0.004	0.245	0.153	**-0.570**	**-0.467**	-0.177	-0.332
OS										**0.721**	-0.138	0.004	**0.742**	0.234	0.244	0.188
Tacids											-0.031	0.230	**0.352**	0.295	0.086	0.131
O_3												**0.572**	-0.283	**-0.574**	**0.482**	-0.152
NOx													-0.200	-0.086	0.287	-0.035
Temp														0.272	0.238	0.242
RH															**-0.498**	**0.618**
Radiation																**-0.492**

Table 3. Seasonal statistics of measured groups of compounds.

	Spring				Summer				Fall			
(ng/m^3)	mean	median	min	max	mean	median	min	max	mean	median	min	max
Nitro-aromatics	0.07	0.00	ND	0.81	0.02	0.02	ND	0.04	0.28	0.17	0.04	1.78
Organo-sulfates[1]	96.77	83.05	33.07	255.17	153.36	125.41	38.93	306.66	34.69	15.27	0.17	118.68
Terpenoic acids	325.62	304.05	128.68	771.16	294.01	249.19	115.08	634.99	250.66	148.91	52.94	809.46
% of OM[2]												
%Nitro-aromatics	0.00	0.00	ND	0.02	0.00	0.00	ND	0.00	0.01	0.01	0.00	0.02
%Organo-sulfates	2.47	2.42	1.19	3.64	3.87	3.80	1.95	5.56	0.98	0.63	0.31	2.21
% Terpenoic acids	8.65	8.29	4.62	12.88	7.50	7.77	3.80	11.64	6.48	5.21	2.70	12.00

[1] including nitrooxy-organosulfates; [2]Fraction of each group of identified compounds (combined total) to organic matter

Table 4. Ratios of identified nitrogen containing compounds (nitro-aromatics and nitrooxy-organosulfates) to WSON.

	Spring				Summer				Fall			
(ngN/m^3)	mean	median	min	max	mean	median	min	max	mean	median	min	max
WSON	59	74	ND	140	46	33	ND	105	25	15	ND	133
Identified ON	0.48	0.36	0.1	1.75	0.65	0.53	0.12	1.83	0.46	0.26	0.07	1.70
Identified ON/WSON %	1.02	0.64	ND	3.09	2.04	1.71	ND	7.84	4.37	1.50	ND	27.90